

Two-photon cascades of radiative neutron capture. II. Fundamental parameters and features of the gamma decay of compound states of complex nuclei

S. T. Boneva, É. V. Vasil'eva, V. D. Kulik, Le Hong Khiem, L. A. Malov, Yu. P. Popov, A. M. Sukhovoĭ, Pham Dinh Khang, V. A. Khitrov, and Yu. V. Khol'nov
Joint Institute for Nuclear Research, Dubna

M. R. Beitinsh, V. A. Bondarenko, I. L. Kuvaga, P. T. Prokof'ev, and L. I. Simonova
Physics Institute, Latvian Academy of Sciences, Riga

G. L. Rezvaya
Latvian University, Riga

Fiz. Elem. Chastits At. Yadra **22**, 1433–1475 (November–December 1991)

The main features of the system for analyzing the average parameters of cascade γ decay of compound states of complex nuclei are described. Comparison of the calculated and experimentally observed cascade intensities has shown that the partial widths of primary and secondary transitions in nuclei near the $4S$ maximum of the neutron strength function depend on the structure of the levels that they connect for excitations on the order of the neutron binding energy. The features of the cascade γ decay of even–odd nuclei can be understood most simply on the basis of the correlation of the neutron partial widths and part of the radiative partial widths as the presence of single-particle transitions between $4S$ and $3P$ neutron shells. It has also been found that for most of the primary $E1$ transitions in ^{137}Ba and ^{181}Hf the radiative strength function corresponds more to the giant electric dipole resonance model, taking into account the temperature and frequency dependence of its width. Here the observed increase of the radiative strength function in certain primary-transition energy ranges in deformed nuclei is, within the error of the predictions of the quasiparticle–phonon model of the nucleus, correlated with the strength-concentration region of the one-quasiparticle states $K^\pi = 1/2^-$ and $K^\pi = 3/2^-$ of the deformed Woods–Saxon potential.

INTRODUCTION

The ultimate goal of experiments in nuclear physics is to develop a theory or model describing the experimental data sufficiently accurately and ensuring adequate predictive power in unstudied areas of nuclear excitation. This problem has not yet been solved for all the possible states of nuclei excited by γ -transition cascades of neutron radiative capture.

The spectroscopy of individual cascades in the reaction $(n, 2\gamma)$ made it possible to obtain¹ a number of conclusions about the features of the γ decay of complex (primarily deformed) nuclei. Here the essentially random nature of the experimentally observed intensities of individual transitions masks and complicates the study of the features of nuclear γ decay below the nucleon binding energy.

Because of this it is necessary to average the experimentally observed γ -transition energies over a larger or smaller range of nuclear excitations.

The fundamental problem arising in the analysis of the experimental results on cascades from two γ quanta emitted in succession by a nucleus [below we refer to this as the reaction $(n, 2\gamma)$] is that semiconductor γ spectrometers operate with nanosecond resolution. Therefore, it is impossible to determine the ordering of the quanta in the cascades observed in radiative neutron capture. In any range of cascade transition energies $E_1 \pm \Delta E_1$, an example of

which is given in Fig. 1, there are cascades with both primary transitions E_1 and secondary transitions E_2 close in energy ($E_1 \cong E_2$).

Distributions analogous to those shown in Fig. 1 were obtained using the spectrum of the summed amplitudes of coincident pulses [the sum–coincidence (SC) spectrum]. This spectrum for the nucleus ^{181}Hf is shown in Fig. 2. The peaks of this spectrum are formed by those cases of γ detection when the energy of one of the transitions is completely absorbed in one detector, and that of the second is completely absorbed in the other detector. The unavoidable background distribution is excluded sufficiently well from the recorded cascade intensity distributions using background events outside the region where the total cascade energy is recorded.

The procedure for analyzing γ – γ coincidences is described in more detail in Ref. 1.

The cascade intensity $\Delta I_{\gamma\gamma}$ where the energy of one of the quanta falls in the interval ΔE_γ can be written as

$$\begin{aligned} \Delta I_{\gamma\gamma} &= \sum_{i,h} i_{\gamma\gamma}(E_\gamma E_c) \\ &= \sum_{i=1}^n \Gamma_{\lambda i}(E_\gamma) \Gamma_{if}(E_c - E_\gamma) / \Gamma_\lambda \Gamma_i \\ &\quad + \sum_{h=1}^m \Gamma_{\lambda h}(E_c - E_\gamma) \Gamma_{hf}(E_\gamma) / \Gamma_\lambda \Gamma_h. \end{aligned} \quad (1)$$

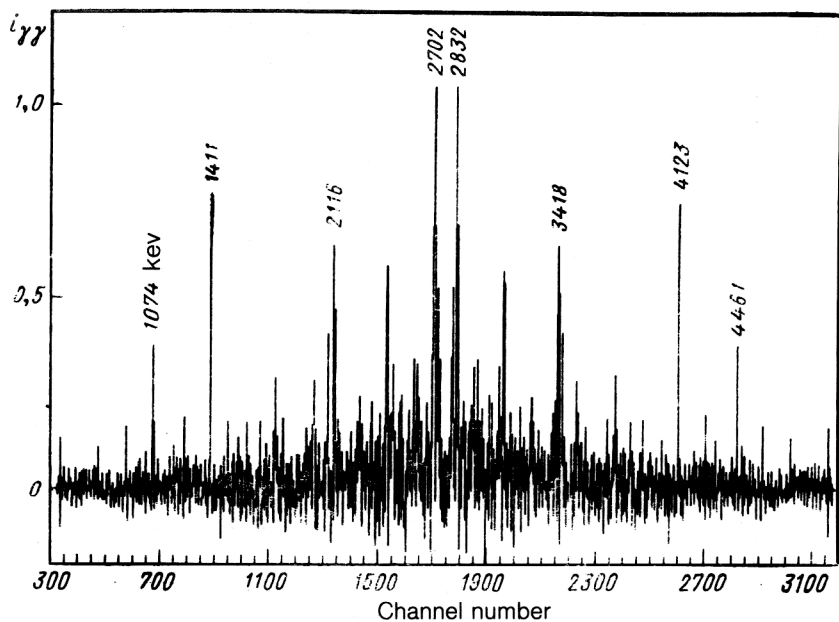


FIG. 1. Distribution of the intensity $i_{\gamma\gamma}$ of cascades to the $J^\pi = 5/2^-$ level of the band of the state $[521]_{1/2}$ in ^{165}Dy . The area of the spectrum is normalized to 100%.

Here $i_{\gamma\gamma}$ is the intensity of an individual cascade with total energy E_c and energy of the quantum (primary or secondary) E_γ ; $\Gamma_{\lambda t}$, $\Gamma_{t(h)}$, $\Gamma_{\lambda h}$, and Γ_{hf} are the partial widths of transitions between the states λ , $t(h)$, and f ; Γ_λ , Γ_t , and Γ_h are the total radiative widths of the levels λ , t , and h ; n and m are the numbers of states excited by primary transitions with energy E_γ and $(E_c - E_\gamma)$, respectively, in the

interval ΔE_γ which is proportional to the level density for a given excitation energy.

An example of a calculated distribution corresponding to Eq. (1) in the absence of any fluctuations of the partial radiative widths of cascade transitions is shown in Fig. 3.

Such distributions, obtained experimentally, represent convolutions of the fundamental parameters of nuclear

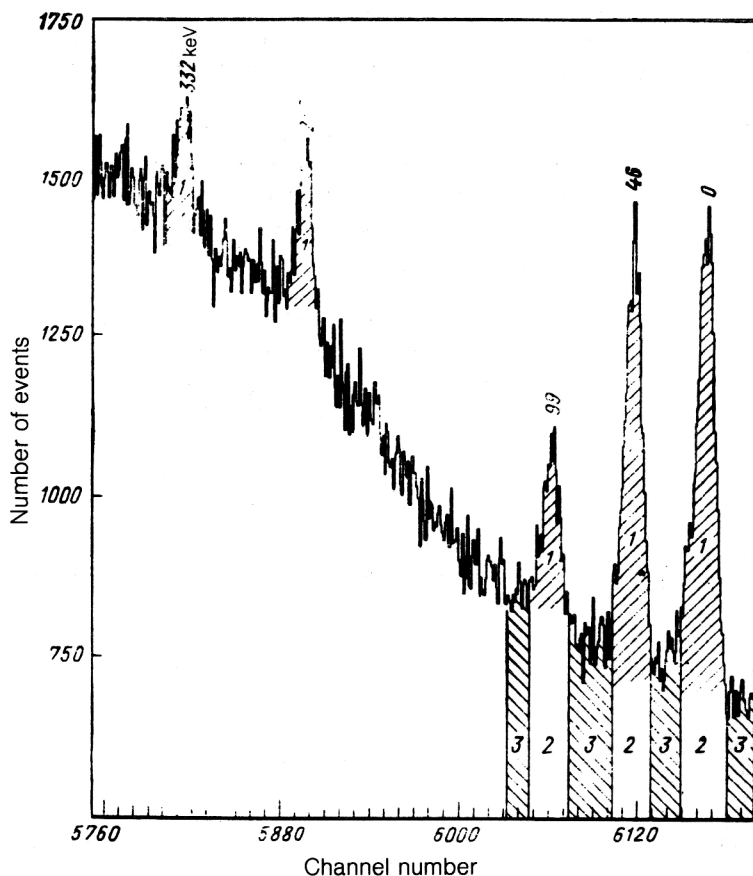


FIG. 2. Part of the SC spectrum for the nucleus ^{181}Hf . Curve 1 corresponds to cases where the total energy of the cascade is detected, 2 corresponds to the background, and 3 corresponds to exclusion of the background distributions.

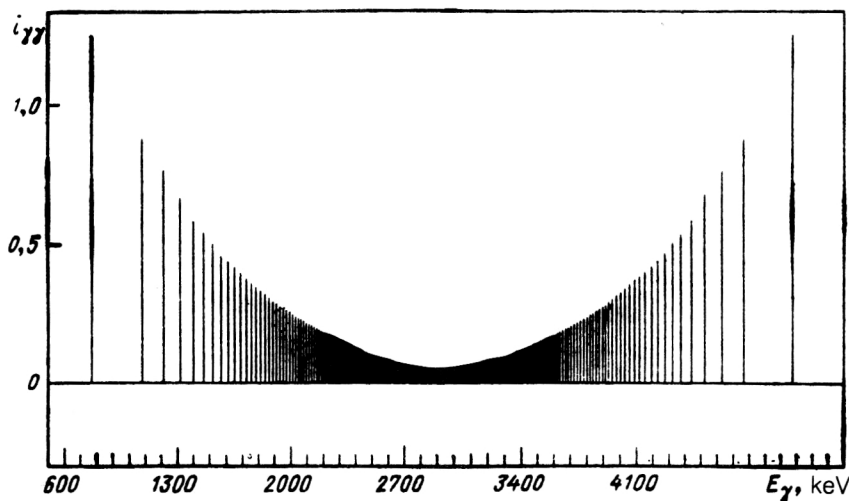


FIG. 3. Calculated distribution of the intensity $i_{\gamma\gamma}$ of cascades to the $J^{\pi} = 3/2^{-}$ level of the state $[521]_{1}^{+}$ of the nucleus ^{163}Dy . The area of the spectrum is normalized to 100%.

models: the radiative strength function (RSF) of the primary (secondary) transitions and the density of states t or h excited by them. The experimental analog of the calculated spectrum (Fig. 3) is shown in Fig. 4.

The shape and nature of the experimentally obtained cascade intensity distributions depend not only on the average γ -decay parameters [Eq. (1)], but also on:

- (a) fluctuations of the widths of the primary and secondary transitions;
- (b) the ratio of the useful and background coincidences, the summed amplitudes of which fall into the given interval,¹ i.e., the ratio of the areas of regions 1 and 2 in the SC spectra (see Fig. 2);
- (c) the finite energy resolution of the detectors.

Comparison of the cascade intensity distributions for the nuclei ^{163}Dy and ^{165}Dy (Figs. 1 and 4) shows that they can differ markedly in shape even in neighboring nuclei of the same type. This fact is not trivial: the total radiative widths of the neutron resonances have a monotonic and weak dependence on the atomic mass of the target nucleus.

In addition, it should be noted that the summed cascade intensities differ from the results of model calculations using Eq. (1), both in cascades to levels of the same structure in neighboring nuclei and in cascades to different final states in the same nucleus.

The extraction and analysis of concrete information on the features of the γ decay of a compound state with nuclear excitation in the energy range up to 8 MeV in this case can be carried out at several levels:

- (a) by comparison of the experimentally observed and theoretically predicted summed intensities of all possible cascades between a compound state and a given level;
- (b) by comparison of the shapes of the distributions of the experimentally obtained spectra and the analogous distributions calculated using Eq. (1) in a sufficiently wide energy range;
- (c) by analysis¹ of the intensity distribution of the experimentally resolved cascades;
- (d) by multiplying the experimental distributions (see Figs. 1 and 4) by the components of the "primary" and

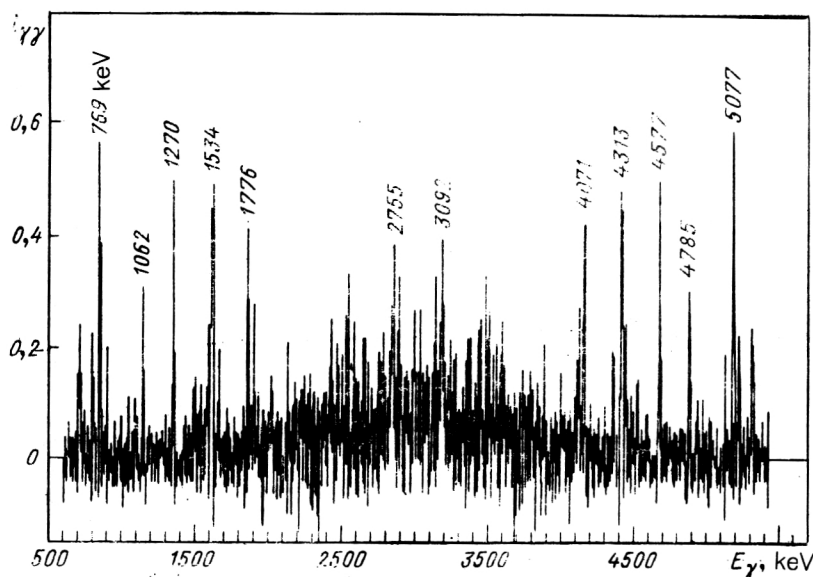


FIG. 4. Observed distribution of the cascade intensity $i_{\gamma\gamma}$, the analog of the calculated distribution shown in Fig. 3.

“secondary” transitions with subsequent (when possible) extraction of information about the density of states excited by primary transitions of the dipole type and, finally, their RSF.

The technique described below for analyzing ordinary γ - γ coincidences was developed at the JINR. It made it possible for the first time ever to begin systematic investigations of the properties of the excited states of complex nuclei in the entire range of excitation energies below the neutron binding energy. Moreover, in principle it allows the solution of the fundamental problem of experiment in this area of nuclear physics: the determination of the RSF of the primary transitions in their entire energy range, which up to now has been inaccessible to the traditional methods of nuclear and neutron spectroscopy.

1. SUMMED INTENSITIES OF TWO-PHOTON CASCADES TO GIVEN LOW-LYING LEVELS

The summation interval in Eq. (1) can be extended to practically the neutron binding energy, and the values obtained can be summed for several final cascade levels.

The resulting intensity $I_{\gamma\gamma}^c$ (% per decay) characterizes the fraction of the total intensity of primary transitions (the total radiative width of the compound state Γ_λ) which is observed experimentally. Naturally, this sum extended to all final cascade levels is 100%. Therefore, actually only deviations from the expected values can appear for particles of the final levels.

The analogous calculated value $I_{\gamma\gamma}^c$ can be determined on the basis of various model representations of the energy dependence of the widths of the primary (secondary) cascade transitions and the density of states excited by them.

Obviously, comparison of different variants of such calculations with experiment makes it possible to determine how the model description of γ decay must be modified to improve its agreement with experiment.

The model description of cascade γ decay

As an example, let us compare the experimental results with the results of calculations using two models of the excited-state density and two models of the partial radiative widths.

A. The “back-shifted” Fermi-gas model for the density of states. The parameters of this model for the nuclear moment of inertia equal to half the rigid-body moment of inertia are given in Ref. 2. The choice of this moment of inertia was suggested by the experimental results given in, for example, Ref. 3.

B. Fermi-gas models taking into account the shell non-uniformities of the single-particle spectrum using the shell correction of V. M. Strutinsky developed in the works of Ignatyuk.⁴

To present a complete picture, here we could include also the combinatorial calculation⁵ of the level density. However, this calculation is very awkward and can be done in a limited number of cases.

A detailed comparison of these three variants of the density of excited states with $K^\pi = 1/2^+$ for ^{165}Dy is given in Fig. 5.

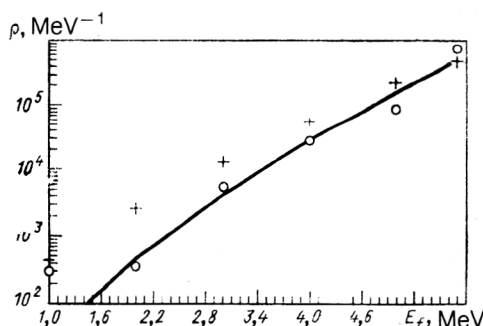


FIG. 5. Calculated density ρ of states with $K^\pi = 1/2^+$ in ^{165}Dy as a function of the excitation energy E_f . The curve is the calculation using the model of Ref. 4, the points + show the calculation using the back-shifted Fermi-gas model with parameters from Ref. 2, and the points O show the combinatorial calculation of Ref. 5.

We see that the level density predicted by model A is higher than that of model B. The combinatorial calculation gives results for this nucleus which coincide with those of the first model at low excitation energies and those of the second at high energies.

In model A the density of excited states is interpolated between two excitation regions: $E_f \lesssim 1$ MeV and $E_f \gtrsim B_n$.

In model B, the variant used below, the parameters can be fitted only for the neutron-resonance density.

It can be assumed that the actual density of excited states will be intermediate between these two cases; the latter will be more accurate if in the calculation of the parameters of model A the experimental level density obtained in the reaction $(n, 2\gamma)$ for $E_i > 1$ MeV is used.

The common feature of all the models of the functional dependence of the level density at the present time is the fact that it has an exponential dependence on the excitation energy. Here the exponential is a smooth function of a large or small number of continuous parameters. It can therefore be expected that a decrease of the excitation-energy interval in which the density of states is specified by extrapolation of the experimental data makes the prediction of this quantity more reliable, for $2 \text{ MeV} < E_i < B_n$.

The situation with the partial widths of the primary and secondary quanta of the radiative decay of a compound state is less certain. The matrix element of the transitions of the most probable multipole orders $E1$ and $M1$ is known in only a limited number of cases: for hard primary transitions to states $E_f \lesssim 2$ MeV for even-even compound nuclei and $E_f \lesssim 1\text{--}1.5$ MeV for even-odd ones.

The number of models predicting the value of this parameter is quite large. However, those of practical interest are primarily the giant electric dipole resonance (GEDR) model for $E1$ transitions and the Weisskopf model, which assumes that the dependence of $\Gamma_{\lambda f}(\Gamma_{if})$ on the transition energy E_γ is proportional to E_γ^{2L+1} , where L is the multipole order of the transition for $M1$ and $E2$ transitions.

Experience in analyzing the experimental data on the reaction $(n, 2\gamma)$ that we have accumulated up to now⁶

shows that the Weisskopf model cannot claim to give a more or less correct description of the dependence $\Gamma_{\lambda t} = f(E_\gamma)$ for $E1$ transitions. The cascade intensities obtained using this model are 2 to 4 times smaller than the experimental values for any model of the level density.

The role of various types of transition in cascade γ decay

The reason for this discrepancy between the calculated and the experimental results is the following: magnetic dipole and electric quadrupole transitions, as will be shown below, play an important role in the decay of low-lying states of a complex nucleus compared with the hard primary transitions of the decay of a compound state, where the fraction of their widths relative to the widths of $E1$ transitions is less than 15–20% for nuclei with $A \gtrsim 140$.

A simple functional dependence $\Gamma_{\lambda t} = f(E_\gamma)$ cannot take this fact into account even in principle, if in the calculation we use the experimental ratios of the widths of hard primary transitions of various multipole orders, which are well known experimentally for many nuclei from the reaction (\bar{n}, γ) .

Meanwhile, as has been established by now for ^{144}Nd (Ref. 7), ^{137}Ba , and ^{181}Hf (see below), in a wide range of soft primary transition energies the RSF depends weakly on the transition energy, as required by the Weisskopf model. Apparently, owing to these features, the combination of GEDR models for $E1$ transitions and the Weisskopf model for $M1$ and $E2$ transitions leads to the smallest discrepancy between the experimental and theoretical results. Here it can be hoped that the experimental study of magnetic dipole transitions will permit the development of a giant magnetic dipole resonance (GMDR) model for low excitation energies in deformed nuclei. This would ensure even greater accuracy in the description of cascade γ decay.

The GEDR and GMDR models (for $M1$ transitions) should be very close to the physical reality observed in the reaction $(n, 2\gamma)$. However, unfortunately, the cross section for absorption of even an electric dipole quantum is experimentally determined for a very restricted number of nuclei and energies if the quantum energy is smaller than the neutron binding energy.

The situation with regard to $M1$ transitions in deformed nuclei, where the GMDR parameters are unknown even for $E_t > B_n$, is even more uncertain.

The general conclusion reached in the study⁸ of electroexcitation of the 1^+ state in even-even nuclei of the deformed region is that the magnetic resonance is strongly fragmented in a wide range of excitations of such nuclei. Meanwhile, in spherical nuclei with $A \approx 100$ its maximum is located in the region $E^* \approx B_n$. At present there is no other information about this resonance.

It should be noted that the reaction $(n, 2\gamma)$ makes it possible to explain the relative role of magnetic transitions in cascade γ decay.

In Sec. 4 we describe a technique for obtaining the dependence $i_{\gamma\gamma} = f(E_1)$ on the energy of the primary $E1$

transition, both for cascades to individual low-lying states and for their sum over final states f .

From the form of the first term in Eq. (1) it is easy to see that the ratio of the cascade intensities, the primary transition energies of which lie in the range $E_1 \pm \Delta E_1$ (and where the final level has a given value of J^π), to the sum, sufficiently complete in f , of intensities of such cascades to any low-lying levels will be $\Gamma_{tf}(E_c - E_\gamma)/\Gamma_t$.

By comparing the cascade γ decay in pairs of compound nuclei such as $^{162,164}\text{Dy}$ and $^{178,180}\text{Hf}$, in which the parity of the compound state is reversed, according to the measured ratios Γ_{tf}/Γ_t it is possible to estimate both the relative intensity and the form of the energy dependence of Γ_{tf} for secondary $E1$ or $M1$ transitions. Here complete information on the dependence of the ratio Γ_{tf}/Γ_t on the excitation energy of the levels t and f can be obtained only by further development of the experimental technique to the point where at least 80–90% of the total intensity of the primary transitions is measured in the intensity distributions of cascades to (at least) several dozen final states of the even-even nucleus. The possibility of reaching this level depends only on technical problems: the need to use a system of many detectors with high efficiency for recording γ - γ and γ - γ - γ coincidences.

At the present time it has already been established that cascades between states of opposite parity ($E1 + M1$ transitions) usually exceed the calculated estimates (or are equal to them), while cascades between states of identical parity usually lie below the calculated values. In this respect ^{180}Hf is unique. For it, cascades from the 5^+ state to the 2^+ , 4^+ , and 6^+ levels have been studied.⁹ In contrast to all the nuclei that we have studied, here the experimental intensities are lower than the calculated ones by at least a factor of 2 (see Ref. 9 and Table II below).

Here it should be noted that, in principle, the currently existing interpretations of the data on the reaction $(n, 2\gamma)$ cannot be taken as definitively established. Many of them need to be checked further. This is not surprising, since many parameters affect cascade γ decay. An illustration of this is given in Table I, where the parameters of the nuclei ^{168}Er , ^{178}Hf , and ^{180}Hf studied by us in the reaction $(n, 2\gamma)$ are compared.

Comparison of the summed cascade intensities for the three nuclei in Table I with the values of $2g\Gamma_n^0$ of resonances determining the neutron-capture cross section, the structure, spin, and parity of the ground state, and, accordingly, the type of transitions involved in the cascade shows that it is impossible to arrive at any unique interpretation of the results with the small set of even-even compound nuclei studied. The partial radiative widths of the cascade transitions in a wide range of excitations of these nuclei depend on the full set of parameters.

As a first approximation, for a preliminary estimate of the expected summed intensities of cascades from two successive transitions we can use the above-mentioned combination of models for the partial widths: the GEDR model plus the Weisskopf model for $M1$ and $E2$ transitions.

The accumulation of information on the shapes of the cascade intensity distributions, on calculated values of the

TABLE I. Some parameters of the nuclei ^{168}Er and $^{178,180}\text{Hf}$ and data on their cascade γ decay.

Parameter	^{168}Er	^{178}Hf	^{180}Hf
Fraction of captures for given spin of the compound state	33% 3^+ + 67% 4^+	60% 3^- and 40% 4^-	100% (5^+)
Binding energy, keV	7771	7626	7388
Average distance between resonances, eV	4.0(2)	2.5(2)	4.4(2)
Sum of observed intensities of cascades to levels of the ground-state rotational band, % per decay	15.4(10)	15.1(7)	4.6(5)
Number N_c of the strongest cascades distinguished	71	136	99
Average intensity of the N_c cascades (decays)	9.8×10^{-4}	6.4×10^{-4}	1.3×10^{-4}
Ground-state structure of the target nucleus	[633] \uparrow	[514] \downarrow	[624] \uparrow
Values of $2g\Gamma_n^0$ of resonances determining the thermal neutron capture cross section (Ref. 10), MeV	0.3 and 0.46	1.81 and 5.82	10.45
Neutron strength function, 10^4	1.8(2)	2.5(2)	1.7(2)

total radiative widths Γ_λ of neutron resonances, and, finally, on the energy dependence of the RSF of primary transitions in the compound nuclei ^{137}Ba and ^{181}Hf (see Sec. 4) requires that the modified GEDR model also be included in the calculations. This model¹¹ takes into account both the frequency and the temperature dependence of the GEDR width.

In Tables II and III we give the values of the cascade intensities $I_{\gamma\gamma}^c$ that we obtained to given low-lying levels E_f of the nuclei studied so far. The value of $I_{\gamma\gamma}$ in these tables is equal to the sum of the intensities of the individual cascades, the energy of the intermediate level of which satisfies the condition $B_n - 0.52 \geq E_i \geq E_f + 0.52$ MeV. The experimental values are compared with the results of four variants of the calculation, combinations of the two level-density models and the two GEDR models. The individual features of the nuclei below the energy $E_f \lesssim 1\text{--}2$ MeV were taken into account by including in the model the experimental decay scheme for the nuclei studied (J^π , E_f , and the branching coefficients). The ratio of the widths of transitions of different multipole order needed in the calculation of Eq. (1) was fixed at the primary transition energy $E_1 \lesssim B_n$ on the basis of the experimental data for the reaction (\bar{n}, γ) , i.e., study of the γ decay of compound states with averaging over the neutron resonances.

We see from Tables II and III that one finds the ratio $I_{\gamma\gamma}^c/I_{\gamma\gamma} \lesssim 2$ for most of the experimental data. Clear exceptions to this rule are cascades to states for which $|J_\lambda - J_f| = 3$.

Change of the spin by 3 units as a result of two γ transitions requires that one transition be purely quadrupole. Since it is difficult to expect a large contribution from $M2$ transitions to decays of relatively low-lying states of interest here, the enhanced cascades in Tables II and III most likely correspond to the first transition being an $E1$ (or $M1$) transition and the second being an $E2$ one. These cascades differ from cascades to other levels only by the presence of the $E2$ transition; the enhancement of the widths relative to the calculated values can be related only to enhancement of secondary $E2$ transitions.

In Sec. 3 below we describe a technique for decomposing the spectral distributions of the intensity into components corresponding to primary and secondary cascade

transitions. In the nuclei studied, ^{137}Ba , ^{146}Nd , ^{174}Yb , ^{181}Hf , and ^{183}W , this decomposition has been done mainly for cascades satisfying the condition $|J_\lambda - J_f| \leq 2$. The exception is cascades to the ground state of ^{146}Nd . For the compound state the spin is $J^\pi = 3^-$, and for the ground state $J^\pi = 0^+$. Therefore, here the most realistic type of transition is that with primary $E1$ quanta and secondary $E2$ quanta.

The cascade intensity distribution obtained by the technique described in Ref. 12 is shown in Fig. 6 as a function of the primary-transition energy. Here the statistical error in determining the cascade intensity is too large, making it impossible to arrive at reliable conclusions. Nevertheless, owing to the regular excess of the experimental values of the intensities over the calculated values, we can draw the preliminary conclusion that the widths of secondary $E2$ transitions considerably exceed the model values in a wide range of excitation energies for this nucleus.

The spread in the ratios of the experimental and calculated intensities in all the nuclei studied with $|J_\lambda - J_f| = 3$ depends on the actual decay scheme of the low-lying states. For example, the fairly good agreement between $I_{\gamma\gamma}^c$ and $I_{\gamma\gamma}$ in the case of ^{175}Yb is attained owing to the cascade with $E_1 = 5627$ keV + $E_2 = 556$ keV, which gives the dominant and practically the only contribution to both the calculated and the experimental value of $I_{\gamma\gamma}$ (and similarly for several nuclei).

On the whole, the data of Tables II and III can be explained only if it is assumed that the values of $\Gamma(M1, E2)$ increase systematically relative to $\Gamma(E1)$ as the excitation energy of the nuclei in question decreases [compared with the ratio $\Gamma(E1):\Gamma(M1):\Gamma(E2) = 1:0.15:0.01$ obtained for hard γ transitions in the reaction (\bar{n}, γ)].

The cascades to the levels $E_f = 602$ and 639 keV in ^{179}Yb , 476 and 518 keV in ^{179}Hf , and 99 keV in ^{183}W should also be noted. In the first two cases cascades are observed to levels with identical $J^\pi = 5/2^-$ but different structure (the main component of the higher-lying level is [512] \uparrow , and that of the lower-lying one is [510] \uparrow). In this case the ratio $I_{\gamma\gamma}$ clearly demonstrates the dependence of the secondary-transition widths Γ_γ on the structure of the final level in a fairly wide range of excitation energies for practically identical excitation energy and J^π .

TABLE II. Experimental ($I_{\gamma\gamma}^e$) and calculated ($I_{\gamma\gamma}^c$) intensities of cascades to low-lying levels E_f of even-even nuclei, % per decay.

Nucleus, fraction of captures with given J^π	E_f , keV	Probable type of transitions in the cascades**	$I_{\gamma\gamma}^e$	$I_{\gamma\gamma}^c$ models:			
				GEDR with $\Gamma_G = \text{const}$		GEDR with $\Gamma_G = f(E_\gamma T)$ (Ref. 11)	
				A	B	A	B
^{144}Nd $\approx 100\%$ 3^-	0	$E1 + E2$	3,7(10)	3,8	5,1	3,4	5,1
	696	$E1 + M1$	32,0(30)	12,4	13,2	10,0	12,7
	1314	$E1 + M1$	7,3(14)	6,6	7,5	5,6	6,5
	1510	$E1 + E1$	3,9(10)	7,5	8,6	5,4	6,6
	1561	$E1 + M1$	(2,8)***	3,0	3,2	2,7	2,8
^{146}Nd $\approx 100\%$ 3^-	0	$E1 + E2$	3,9(2)	0,5	0,8	0,5	0,7
	454	$E1 + M1$	19,8(5)	9,5	11,4	8,4	11,2
	1043	$E1 + M1$	5,1(7)	5,9	7,6	4,9	6,8
	1189	$E1 + E1$	7,2(8)	6,6	8,1	4,7	6,3
^{168}Er 33% 3^+ 67% 4^+	80	$E1 + E1$	4,6(4)	3,0	3,6	2,1	2,7
	264	$E1 + E1$	7,7(8)	5,2	6,8	3,4	5,0
	549	$E1 + E1$	3,1(2)	0,9	1,3	0,8	1,0
	821	$E1 + E1$	2,8(4)	1,1	1,6	0,8	1,3
	896	$E1 + E1$	5,4(9)	1,8	1,8	1,3	2,2
	995	$E1 + E1$	3,1(12)	1,7	2,9	1,2	2,1
^{174}Yb 36% 3^- 64% 4^-	0	$E1 + E2$	3,4(3)	1,2	1,3	1,0	1,2
	76	$E1 + M1$	11,8(6)	8,1	8,6	7,0	7,9
	253	$E1 + M1$	6,6(6)	4,9	5,3	4,2	4,8
^{178}Hf 60% 3^- 40% 4^-	0	$E1 + E2$	0,5(2)	0,2	0,4	0,2	0,3
	93	$E1 + M1$	7,5(5)	3,1	3,9	2,5	3,5
	306	$E1 + M1$	6,5(4)	3,8	5,0	3,0	4,3
	632	$E1 + M1$	(0,6)***	0,5	0,8	0,4	0,6
	1174	$E1 + M1$	0,5(2)	0,6	1,0	0,5	0,8
	1267*	$E1 + M1$	1,8(5)	1,9	3,4	1,5	2,8
^{180}Hf $\approx 100\%$ 5^+	93	$M1 + E2$	0,6(1)	0,2	0,3	0,4	0,5
	308	$E1 + E1$	2,3(4)	5,1	5,7	3,8	4,7
	641	$E1 + E1$	1,7(3)	3,5	4,6	2,6	3,7
	1370*	$E1 + E1(M1)$	1,3(4)	1,7	2,7	1,4	2,3
	1430	$E1 + M1$	0,6(3)	0,4	0,6	0,4	0,5
	1482	$E1 + M1$	1,2(4)	1,1	2,0	0,9	1,5
	1610*	$E1 + M1(E1)$	1,8(4)	2,0	3,9	1,7	3,1

*The multiplet.

**A mixture of $M1$ and $E2$ transitions and cascades with opposite ordering of the photons are also possible.

***An estimate of $I_{\gamma\gamma}^c$.

In the last case, ^{183}W , the intensity of cascades to the level with $J^\pi = 5/2^-$ of the rotational band of the state $[510]\uparrow$ is considerably smaller than the empirical value (see Table III), and also smaller than the ratio $I_{\gamma\gamma}$ calculated for the $1/2^-$, $3/2^-$, and $5/2^-$ states of this band. This is also correlated with the relative increase in the lifetime of the level with $J^\pi = 5/2^-$.

The general conclusion that we can draw on the basis of Tables II and III is that models which claim to be fairly accurate (to tens of percent) in describing the γ decay of a compound state must be more detailed than the ones presently used. In addition, on the average over the 14 nuclei studied so far, no definite preference can be shown toward any pair of models describing the level density and energy dependence of the radiative-transition probability.

2. A POSSIBLE INTERPRETATION OF THE DISCREPANCY BETWEEN THE EXPERIMENTAL AND CALCULATED CASCADE INTENSITIES

The experimentally observed cascade intensity distributions are distorted by (a) random fluctuations of the widths $\Gamma_{\lambda i}$ and Γ_{if} of the cascade transitions, (b) the "noise" distribution due to the procedure of subtracting the background events (see Ref. 1 and Fig. 2), and (c) the finite resolution of the detectors used in the experiments.

The shape of the intensity distributions expected in the absence of these distortions is shown in Fig. 3.

The calculated and experimental distributions can be summed over a fairly wide excitation-energy range (for example, 100 keV). By comparing them it is possible to

TABLE III. Experimental and calculated intensities of cascades in the even-odd compound nuclei studied, % per decay.

Compound nucleus	E_f , keV	Probable type of transition in the cascades***	$I_{\gamma\gamma}^e$	$I_{\gamma\gamma}^c$ models			
				GEDR with $\Gamma_G = \text{const}$		GEDR with $\Gamma_G = f(E_\gamma T)$ (Ref. 11)	
				A	B	A	B
^{137}Ba	0	$E1 + E1$	15,5(7)	27	27	21	21
	281	$E1 + E1$	53(3)	20	20	16	16
	1900	$E1 + E1$	(2,2)****	1,6	1,7	1,7	1,7
	2180	$E1 + M1$	(1,6)****	1,0	1,1	1,1	1,1
^{163}Dy	0	$E1 + M1$	5,9(4)	4,2	4,8	3,2	3,8
	73	$E1 + E2$	1,1(2)	0,06	0,09	0,05	0,08
	251	$E1 + E1$	2,7(2)	2,7	3,6	2,0	2,6
	351*	$E1 + M1$	5,2(4)	4,1	4,9	3,2	4,1
	390*	$E1 + M1$	4,9(9)	3,7	4,5	3,0	3,7
	422+428*	$E1 + M1$	6,3(11)	5,1	6,3	4,0	5,3
	475	$E1 + M1$	1,5(6)	1,5	2,0	1,2	1,7
^{165}Dy	0	$M1 + E2$	(1,8)****	0,02	0,04	0,02	0,04
	108*	$E1 + M1$	11,0(19)	7,8	8,8	6,3	7,5
	158*	$E1 + M1$	11,5(25)	7,1	8,3	5,7	7,1
	181+185*	$E1 + M1$	9,8(23)	6,5	7,6	5,3	6,6
	533+538	$E1 + M1$	7,4(25)	4,8	8,3	4,0	6,6
	570+573	$E1 + M1$	12,7(48)	5,4	8,6	4,6	7,7
^{175}Yb	0	$E1 + E2$	2,9(4)	0,9	1,5	0,7	1,2
	515*	$E1 + M1$	17,2(40)	7,4	8,4	6,0	6,9
	556*	$E1 + M1$	18,1(47)	6,7	7,8	5,4	6,5
	602*	$E1 + M1$	9,0(16)	3,1	3,7	2,5	3,1
	639	$E1 + M1$	2,3(16)	2,8	3,5	2,3	2,9
	811**	$E1 + M1$	11,5(59)	3,5	4,8	3,0	4,1
	871**	$E1 + M1$	2,3(13)	1,5	2,2	1,3	1,9
	920	$E1 + M1$	6,3(37)	2,7	3,9	2,3	3,4
	992	$E1 + M1$	3,4(13)	2,2	2,2	2,0	3,0
^{177}Yb	332*	$E1 + M1$	21,9(33)	10,5	11,1	8,6	9,2
	376*	$E1 + M1$	20,9(26)	8,3	8,1	6,9	7,0
	423*	$E1 + M1$	15,7(31)	4,8	5,1	3,9	4,2
^{179}Hf	214	$E1 + E2$	2,1(9)	0,03	0,04	0,03	0,03
	375*	$E1 + M1$	15,5(16)	5,8	6,3	4,6	5,2
	421*	$E1 + M1$	16,5(21)	5,4	5,9	4,3	4,9
	476*	$E1 + M1$	7,6(6)	3,0	3,6	2,4	2,9
^{179}Hf	518	$E1 + M1$	4,0(8)	2,7	3,3	2,1	2,7
	614	$E1 + M1$	9,5(16)	4,1	4,8	3,3	4,0
	679	$E1 + M1$	3,8(8)	3,5	4,1	2,8	3,5
	701	$E1 + M1$	2,6(5)	1,7	2,1	1,4	1,8
	721**	$E1 + M1$	3,1(7)	3,2	3,8	2,6	3,2
	788**	$E1 + M1$	2,7(8)	1,4	1,8	1,2	1,5
^{181}Hf	0*	$E1 + M1$	15,2(20)	10,5	11,3	8,4	9,2
	46*	$E1 + M1$	15,6(20)	11,0	12,6	8,8	10,1
	99*	$E1 + M1$	8,9(20)	5,2	5,7	4,2	4,7
	252**	$E1 + M1$	8,0(13)	6,8	7,1	5,5	6,0
	332**	$E1 + M1$	4,1(10)	3,3	3,6	2,7	3,0

TABLE III. (Continued.)

Compound nucleus	E_f , keV	Probable type of transition in the cascades***	$I_{\gamma\gamma}$	$I_{\gamma\gamma}$ models			
				GEDR with $\Gamma_G = \text{const}$		GEDR with $\Gamma_G = f(E_\gamma, T)$ (Ref. 11)	
				A	B	A	B
^{183}W	0*	$E1 + M1$	13,3(11)	8,7	9,4	6,9	7,6
	46*	$E1 + M1$	10,2(7)	8,7	9,8	6,9	7,9
	99*	$E1 + M1$	1,4(2)	3,9	4,2	3,1	3,4
	209**	$E1 + M1$	8,1(19)	6,5	7,2	5,2	6,0
	292**	$E1 + M1$	4,3(6)	3,0	3,3	2,4	2,7
^{187}W	0**	$E1 + M1$	12,6(13)	9,1	10,4	7,4	8,6
	77**	$E1 + M1$	5,6(5)	4,0	4,6	3,3	3,8
	146*	$E1 + M1$	9,5(10)	6,3	7,1	5,2	5,9
	205*	$E1 + M1$	10,7(6)	6,0	6,7	5,0	5,7
	303*	$E1 + M1$	5,1(10)	2,5	2,9	2,1	1,5

*Levels of the rotational band of the state $[510]\uparrow$; for ^{165}Dy those of the state $[521]\downarrow$.

**Levels of the rotational band of the state $[512]\downarrow$.

***In cascades with the most likely multipole order $E1 + M1$ an admixture of the $E2$ component for $J^\pi = 3/2 \pm$ is possible. Reversed ordering of the transitions in the cascade is not excluded.

****An estimate of $I_{\gamma\gamma}^e$

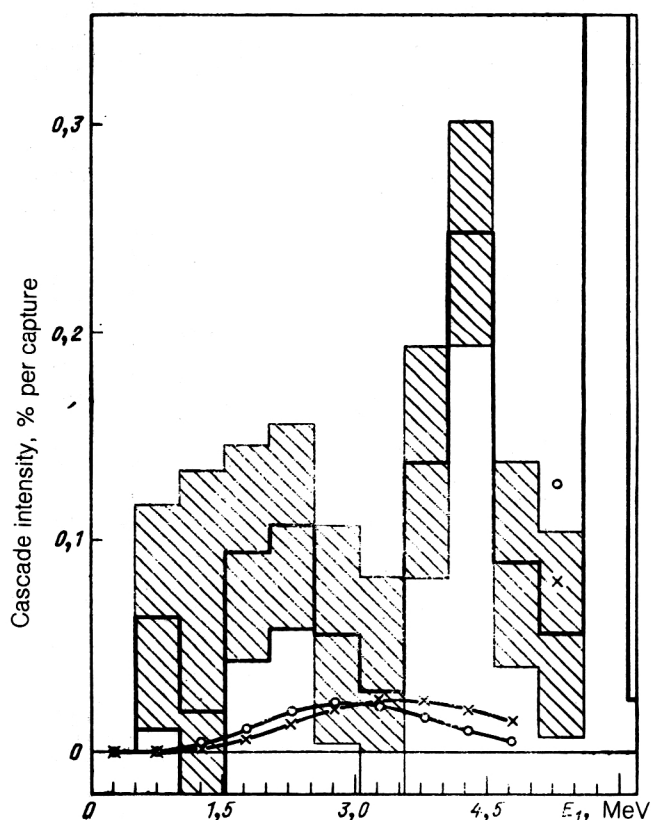


FIG. 6. Intensity of cascades to the ground state of ^{146}Nd . The histogram is from experiment, the statistical errors are shaded, \circ are calculated using the model of Ref. 4, \times are calculated using the model of Ref. 2.

find the range of cascade γ -transition energies where enhancement of the intensities is observed. The most important result, obtained by us earlier⁶ in nuclei such as ^{165}Dy and ^{168}Er , is that the summed intensities of cascades via intermediate levels with energy $E_f \approx 0.5B_n$ in certain energy ranges are significantly enhanced relative to the average calculated values. No noticeable discrepancies between the calculation and experiment were observed for low energies of the cascade quanta.

Direct comparison of the experimental spectral distributions with their calculated analogs is not useful at present and will not be discussed here.

In Sec. 3 we describe a technique for decomposing the distributions described by Eq. (1) into the primary and secondary transition components, which gives more useful results.

The simplest explanation of the observed discrepancies between the calculated and experimental cascade intensities is obtained for even-odd compound nuclei in the rare-earth region. These nuclei belong to the $4S$ maximum of the neutron strength function. Therefore, according to, for example, Ref. 11, in the structure of the compound state the weight of the one-quasiparticle components is large relative to the three-, five-, etc., quasiparticle terms in the wave function. The low-lying levels of these nuclei excited by a two- γ cascade have the simplest structure. According to the calculations using the quasiparticle-phonon model,¹³ the principal states of the bands to which the strongest cascades are observed have a structure in which the one-particle components have large weights:

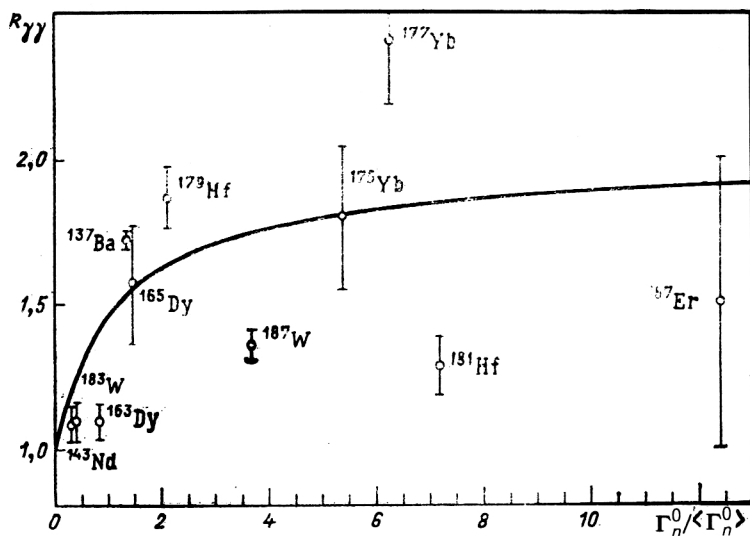


FIG. 7. Ratio $R_{\gamma\gamma}$ of the experimental and calculated summed cascade intensities in a group of even-odd compound nuclei as a function of the ratio $\Gamma_n^0 / \langle \Gamma_n^0 \rangle$ of resonances determining the thermal-neutron capture cross section. The result for ^{143}Nd is from a preliminary processing of the experimental data.

$^{165}\text{Dy}: [521] \downarrow 97\%$,

$^{175}\text{Yb}: [510] \uparrow 85\%$,

$[512] \downarrow + Q_1(22)8\%$, $[512] \uparrow + Q_1(22)7\%$,

$^{179}\text{Hf}: [510] \uparrow 90\%$, $[512] \downarrow + Q_1(22)10\%$,

$^{181}\text{Hf}: [510] \uparrow 95\%$, $[512] \downarrow + Q_1(22)5\%$,

$^{183}\text{W}: [510] \uparrow 90\%$, $[512] \downarrow + Q_1(22)4\%$.

This also leads to our proposed explanation of the enhancement of the cascade intensity: enhanced one-particle transitions between the $4S$ and $3P$ neutron shells are observed experimentally.

The amplitude of the electromagnetic $E1$ ($M1$) transition between states λ and t with complicated structure can be expressed¹⁴ in terms of the one-quasiparticle, three-quasiparticle, quasiparticle \otimes phonon, etc., components of the wave functions of these levels as follows:

$$\begin{aligned}
 M_{\lambda t} \{E1(M1), [J_\lambda^\pi \rightarrow J_t^\pi]\} \\
 = \sum_{\rho_\lambda \rho_t} C_{\rho_\lambda} C_{\rho_t} V_{\rho_\lambda \rho_t} P_{\rho_\lambda \rho_t} + \sum_{\rho_\lambda \rho_t g_\lambda g_t} (C_{\rho_\lambda} D_{g_\lambda} \\
 + C_{\rho_t} D_{g_t}) M_{g_\lambda g_t} + \sum_{g_\lambda g_t} D_{g_\lambda} D_{g_t} P_{g_\lambda g_t} \\
 + \sum_{g_\lambda g_t G_\lambda G_t} (D_{g_\lambda} E_{G_\lambda} + D_{g_t} E_{G_t}) M_{G_\lambda G_t} \\
 + \sum_{G_\lambda G_t} E_{G_\lambda} E_{G_t} P_{G_\lambda G_t} + \dots
 \end{aligned} \quad (2)$$

Here C_ρ , D_g , and E_G are the amplitudes of the wave-function components corresponding to the quasiparticle, the quasiparticle \otimes phonon, and the quasiparticle \otimes two phonons, and P and M are the matrix elements of $E1$ and $M1$ transitions. The detailed calculation of the partial widths using this expression is a difficult and essentially unsolved problem. Nevertheless, it is possible to single out param-

eters on which the width of the transition between the compound state λ and the intermediate level t must depend. These are C_ρ , the amplitude of the one-particle component of the wave function of the compound state, and $V_{\rho_\lambda \rho_t} = u_{\rho_\lambda} u_{\rho_t} - v_{\rho_\lambda} v_{\rho_t}$, the term depending on the coefficients u_ρ and v_ρ in the canonical Bogolyubov transformation for states ρ_λ and ρ_t coupled by a γ transition.

If the experimentally observed enhancement of the cascade intensity can be related to these quantities, it will thereby be possible to see whether the single-particle components contribute significantly to the widths of the experimentally observed transitions.

In the analysis we must take into account the following.

a. The cascade intensity is determined by the width ratio $\Gamma_{\lambda t} / \Gamma_\lambda$. It is therefore necessary to take into account the positive correlation of the random quantities $\Gamma_{\lambda t}$ and $\Gamma_\lambda = \sum_i \Gamma_{\lambda i}$ which can be fairly large.

b. The summed intensities of the cascades from two transitions to all possible final excited states is 100%. The enhancement of any transitions $\lambda \rightarrow t$ must therefore correspond to a decrease of the widths of transitions $\lambda \rightarrow h$, where $h \neq t$. For $\Gamma_\lambda \cong \text{const}$ (an experimental result), this requires an absolute decrease of the widths $\Gamma_{\lambda h}$ for an absolute increase of $\Gamma_{\lambda t}$. The expected relation does actually exist.

In Fig. 7 we show the ratio $R_{\gamma\gamma}$ of the sums of the experimentally observed cascades $\sum_i J_{\gamma\gamma}^e$ to the analogous quantity calculated using the approach described in Ref. 1 (for uniformity we used model B for the level density and the GEDR model with fixed width Γ_G) as a function of the degree to which the compound state is a one-quasiparticle state. The latter is most conveniently represented as the ratio of the reduced neutron width of the resonance Γ_n^0 corresponding to thermal-neutron capture and the average for a given nucleus, $\langle \Gamma_n^0 \rangle = S_0 D_0$.

It follows from point (a) above that the expected relation between $R_{\gamma\gamma}$ and $\Gamma_n^0 / \langle \Gamma_n^0 \rangle$ cannot be linear. If we restrict ourselves to the assumption that the primary tran-

sitions in the decay of a compound state of an even-odd deformed nucleus fall into two groups with widths (a) correlated and (b) uncorrelated with Γ_n^0 of the compound state, we can obtain an analytic expression relating $R_{\gamma\gamma}$ and $\Gamma_n^0/\langle\Gamma_n\rangle$:

$$R_{\gamma\gamma} = (1 + k\alpha\Gamma_n^0/\langle\Gamma_n\rangle)/(1 + k\Gamma_n^0/\langle\Gamma_n\rangle), \quad (3)$$

where the parameters k and α are determined by the ratio of the fractions Γ_λ , coupled to both the correlated and the uncorrelated widths, and also by the coefficient relating the growth of Γ_λ with increasing Γ_n^0 . Of course, this dependence can be taken as only a very crude approximation. This follows both from the fact that the values of k and α can, and most likely do, differ for different nuclei, and from the more complicated relation between Γ_λ and Γ_n^0 than that given by the approximation of the two-component nature of the widths made above. In spite of the very approximate nature of this crude analysis, the relation between the experimental values of $R_{\gamma\gamma}$ and the estimate (3) is quite definite, as can be seen from Fig. 7. Here the parameters k and α lie in the range of the physically allowed values.

The spread in the values of $R_{\gamma\gamma}$ relative to the proposed functional dependence $R_{\gamma\gamma} = f(\Gamma_n^0/\langle\Gamma_n\rangle)$ here is still large. This can be partially explained by the fact that the parameters k and α of the functional dependence (3) cannot remain constant as A is changed. It can also be partially explained by the fact that the calculated cascade intensities are sensitive to the degree of completeness of the data on the decay modes and the parameters of the low-lying levels.

For ^{181}Hf it can also be shown that in this nucleus there are anomalously intense ($\Sigma I_\gamma = 27\%$ per decay) direct transitions to its ground and first excited states, which we did not observe, owing to our experimental conditions (only cascades above the threshold 520 keV were detected).

Under conditions where Γ_λ of the compound state varies weakly for different resonances, the enhancement of some transitions must correspond to the weakening of others. This fact is apparently also responsible for the relatively small value of $R_{\gamma\gamma}$ for ^{181}Hf . On the whole, the data of Fig. 7 should be viewed as qualitative confirmation of the hypothesis that some of the partial widths of primary transitions are correlated with Γ_n of the compound state. This dependence should be studied quantitatively for different resonances of a single nucleus.

The matrix element of the transition (2) depends on the values of the components of the wave functions of the states connected by the γ transition. It is well known, for example, from calculations using the quasiparticle-phonon model (QPM) of the nucleus, that any state of a given structure in real nuclei is fragmented into an entire series of levels. These calculations¹⁴ show that (a) most of the strength of a given state is usually concentrated in some excitation-energy interval of the nucleus on several of its levels, and (b) the regions of the concentrations are located at different nuclear excitation energies, and part of the strength of the state is smeared in a large range of excitation energies.

The assumption that in the cascade decay of compound states of deformed nuclei enhanced transitions are observed with widths determined by the structure of the levels that they connect leads to the conclusion that these transitions should be observed only for certain nuclear excitation energies. Here the clear enhancement of Γ_λ relative to the average value $\langle\Gamma_\lambda\rangle$ should, within the accuracy of the QPM predictions, correspond to the region in which the strength of the one-particle state is concentrated.

In Figs. 8–11 we compare the calculated strength distributions of the fragmented states $[510]\uparrow$, $[521]\downarrow$, $[501]\uparrow$, $[501]\downarrow$, and $[512]\downarrow$ with the values of the cascade intensities (and also hard direct transitions to low-lying levels) for ^{165}Dy , ^{175}Yb , ^{179}Hf , and ^{187}W .

In the histograms of the sums ΣI the intensities of transitions corresponding to excitation of the known low-lying states with $N = 5$ listed above are shaded. We see that the large value of the parameter $(\text{Cu})_{\rho}^2$, which can be viewed as a measure of the concentration of the one-quasiparticle state, here corresponds to a higher value of the primary-transition intensity. The other maxima of the cascade intensity sums (i.e., the maxima Γ_λ) correspond, within the error typical of the QPM (several hundred keV), to the maxima of the calculated strength of the states $[501]\uparrow$, $[501]\downarrow$, $[521]\downarrow$, and $[510]\uparrow$.

It is important that the experimentally observed cascade intensities exceed the values obtained assuming that the primary-transition matrix elements are constant in precisely those nuclei for which Γ_n^0 is larger than the average value. Only the intensity maxima corresponding to primary transitions to states with the structure $[Nn_z\Lambda]\Sigma = [512]\downarrow$ are not observed. The reasons for this are not clear. We can only note that enhancements of the intensities of transitions to levels $[512]\downarrow$ are not observed, both in the case of primary transitions (Figs. 8–11) and in the case of cascades (Table III).

It should also be noted that the values of the observed effects (Figs. 8–11) are different in different nuclei. Here the degree to which the cascade intensity at a given excitation energy exceeds the expected calculated value is related to the degree to which the summed cascade intensities exceed their calculated values (see Fig. 7).

It can be assumed that the experiments and their analysis carried out so far allow us to explain only some of the parameters which describe the γ -decay process.

In summary, we can conclude that both the shape of the cascade intensity distribution and the absolute value of it are determined by the structure of three states: the “initial,” the “intermediate,” and the “final” states connected by the cascade in the excitation-energy interval $E_i = B_n$. This is clearly seen for even-odd compound nuclei. At present it is not possible to draw such a definite conclusion for even-even nuclei, mainly owing to the large number of parameters needed to describe the γ decay (the parities and spins of the compound state and the structure of the low-lying cascade levels) (see Table I).

Nevertheless, in even-even compound nuclei clear deviations of the cascade intensity from the expected values are seen. This is quite clearly observed in the data given in

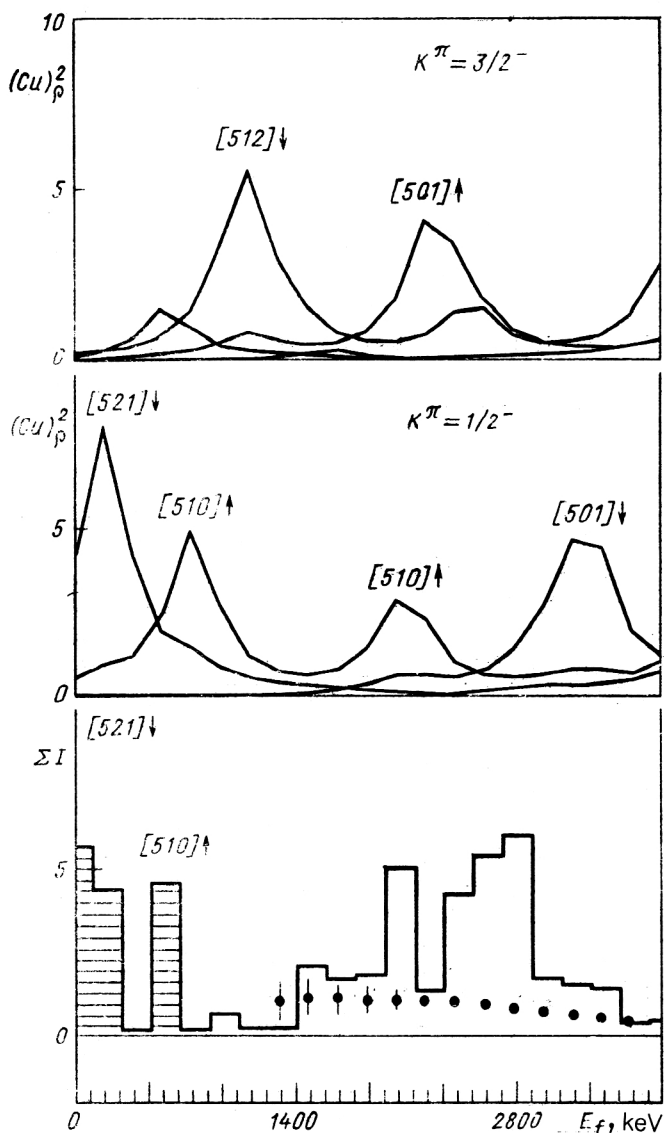


FIG. 8. Distribution of sums ΣI of experimentally distinguished intensities of primary direct and cascade transitions and distribution of the strength $(Cu)_\rho^2$ of fragmentation of one-quasiparticle states as a function of the excitation energy E for the nucleus ^{165}Dy . The histogram is from experiment (% per decay), and the solid lines are the calculation of the fragmentation of states with given values of K^π (relative units). The maxima are labeled with the values of the asymptotic quantum numbers $[Nn_A]\Sigma$. The direct transitions to levels of known structure are shaded, and the points are the statistical calculation of the values of ΣI with the expected random fluctuations.

Figs. 14 and 15, where we show the experimentally measured and calculated cascade intensity as a function of the energy of the primary transition of the cascade for ^{174}Yb .

If we assume that the expected fluctuations in the intensity of an individual cascade about its average value are described by the convolution of two Porter–Thomas distributions (with variance $\sigma_{\text{PT}}^2 = 8$), the expected random fluctuations of the summed cascade intensities can exceed $\sigma_{\text{PT}} = 20\%$ only when the averaging interval (in this case, 500 keV) contains less than $\nu = 200$ cascades (the variance of the sum is $\sigma_{\text{PT}}^2 = 8/\nu$).

The calculations show that in this case this is possible for a primary-transition energy greater than 4.2 MeV. Accordingly, the deviations of the experimental intensities from the expected values for a primary-transition energy of 3.7 MeV (see, for example, Figs. 14 and 15) are not random.

3. THE PROCEDURE FOR DECOMPOSING THE EXPERIMENTAL CASCADE INTENSITY DISTRIBUTIONS INTO TWO COMPONENTS

The intensity distributions of cascades between a compound state and a given low-lying level in any energy interval ΔE_γ in the vicinity of E_γ are the summed intensities of cascades for which the transition E_γ is either primary or secondary. This follows from Eq. (1).

The main assumption used as the basis for decomposing the cascade intensity into two components is the following: the continuous distribution in the cascade intensities remaining after the elimination of the intense, experimentally resolved peaks is caused by the excitation of a large number of intermediate states at excitation energy $E_i > 0.5B_n$. The ordering of the quanta in the isolated intense cascades is determined case by case, mainly using an independent algorithm for constructing the decay scheme¹ in the reaction $(n, 2\gamma)$ (the primary transition of cascades having a common intermediate state and ending at different final levels has the same energy in different spectra). Also, all the available information on the decay modes and energy of the excited states from the reactions (\bar{n}, γ) , (d, p) , (d, t) , $(n, n'\gamma)$, and so on, is taken into account.

The practical threshold for the observation of strong, experimentally resolved cascades with detectors of 10% efficiency is actually $(3-5) \times 10^{-4}$ cases per decay of a compound state and decreases very rapidly with increasing efficiency of the detectors used.

The fraction of cascades resolved experimentally in the form of pairs of peaks amounts to at least 50–70% and more of the full sum of the observed intensity. The remaining undetected 30% (or at most 50%) of the total cascade intensity is formed by the continuous distribution, the main part of which pertains to the region of cascade transition energies near half the cascade energy.

There is no difficulty in subtracting from the experimental intensity distribution several tens of narrow (several keV) peaks. Naturally, the accuracy of this procedure depends on the quality of the spectrum, i.e., on the “noise” fluctuations related to the background-subtraction procedure in obtaining the experimental intensity distributions (see Figs. 1, 2, and 4).

The latter uniquely depend on the ratio of useful and background events in the sum-coincidence spectra (the areas of regions 1 and 2 in Fig. 2). The experimentally required ratios can be reached and exceeded using techniques which have been developed to improve the line shape of semiconductor detectors: anti-Compton shielding, rejection of coincidences in the spectrometer tracks, and so on.

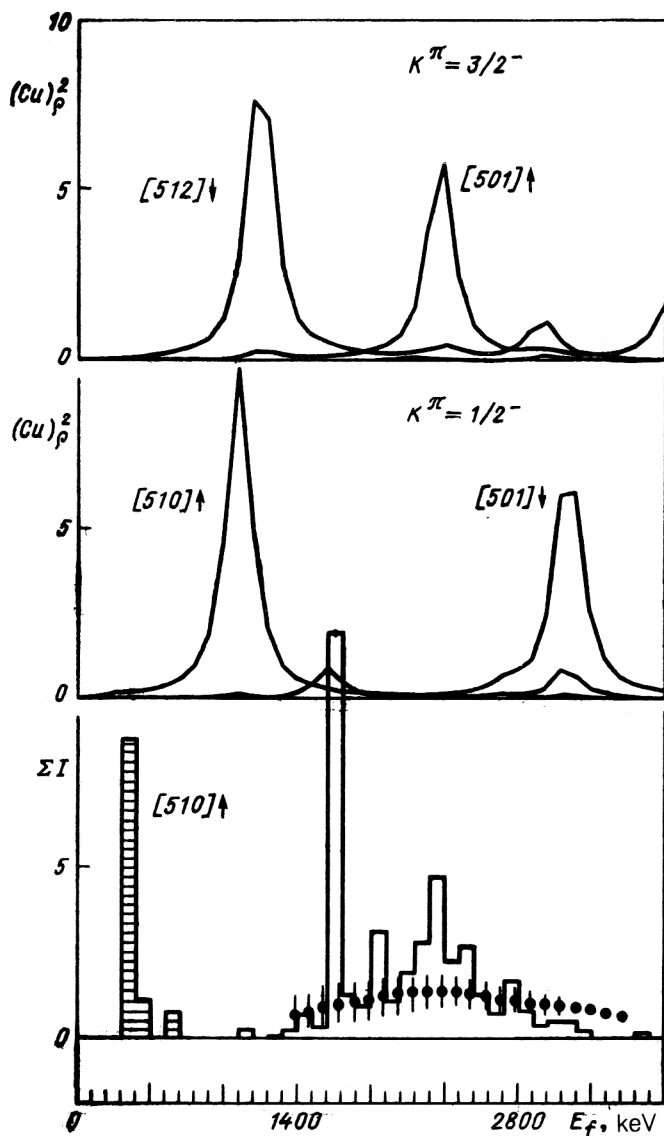


FIG. 9. The same for ^{175}Yb .

The process of decomposing the cascade intensities into the primary and secondary transition components is illustrated in Fig. 12.

At the present time, experimental cascade intensity distributions of the type shown in Figs. 1 and 4 are decomposed into primary and secondary transition components in the following manner.¹²

a. Each spectrum is split into three parts: a central one of width less than 1.5 MeV, and the low- and high-energy ends.

b. Peaks related to the detection of secondary transitions of intense cascades known and determined by us are eliminated from the low-energy part of the spectrum.

c. Only peaks related to the detection of high-energy primary transitions are kept in the high-energy part of the spectra (see Figs. 1, 3, and 12), and the continuous distribution is eliminated.

d. In the central part of the spectrum, half of its intensity is ascribed to primary and half to secondary cascade transitions. The presence of this uncertainty in the processing technique is related only to a deficiency of the detectors

used, which at present do not permit the resolution of a sizable number of cascades of low intensity. At a cascade energy $E_c \gtrsim 6$ MeV the relative width of the incorrectly resolved central part of the spectrum depends rather weakly on the conclusions drawn at in analyzing the cascade intensity distributions as a function of their primary-transition energy. This follows, in particular, from the fact that the "statistical" calculation described above is consistent with this view. At other transition energies the problem of systematic errors in the decomposition procedure reduces to the question of how reliably the decay scheme is determined for $E_i \lesssim 3\text{--}4$ MeV.

Questions of the reliability of the decay scheme for a complex-nucleus excitation energy below 3–5 MeV have been studied in Refs. 1 and 16. The studies showed that at an excitation energy below half the neutron binding energy the probability for incorrect determination of the ordering of the quanta in intense cascades is fairly small. [A false level can be expected no more often than once in ten decay schemes obtained in the reaction $(n, 2\gamma)$.]

At low primary-transition energies the cascade inten-

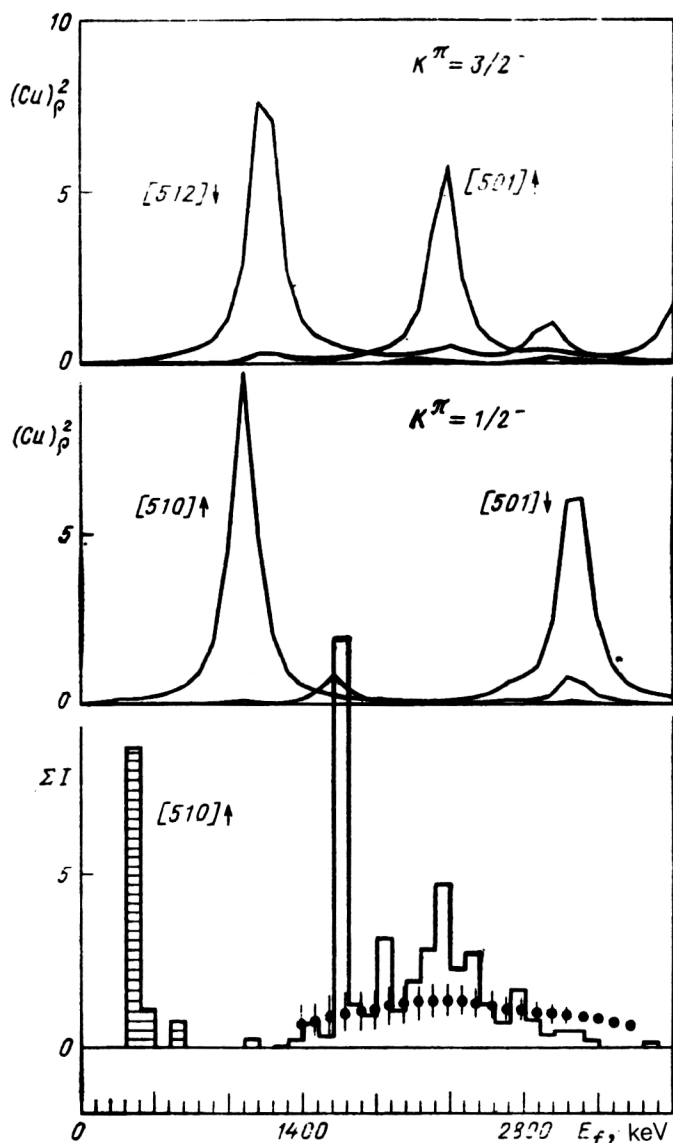


FIG. 10. The same for ^{179}Hf .

sity for the decomposition described here can be overestimated, owing to the following factors.

a. Inclusion of experimentally unresolved cascades of low intensity for which the energy of the secondary quantum is less than 3 MeV.

b. Arrangement of the cascades according to the algorithm of Ref. 1, for which an intense cascade is erroneously shifted in the decay scheme in such a way that a low-energy secondary transition is taken for a primary one.

Since the decay schemes of states excited in the capture of slow neutrons by stable target nuclei in the region of the rare-earth elements are, as a rule, fairly well studied up to excitation energies of 1–2 MeV and sometimes higher, then, in principle, overestimated cascade intensities can arise only for primary-transition energies in the range $1 < E_1 < 3$ MeV.

In nuclei like ^{146}Nd and ^{174}Yb it is difficult to expect an incorrect determination of the cascade intensity for primary-transition energies below 2 MeV for the reasons listed above.

Estimates of the possible systematic error in determin-

ing the cascade intensity for primary-transition energies $E_1 \geq 3$ –4 MeV obtained for the studied nuclei are less than 30% for the experimental results presented below. Such errors are mainly related to weak cascades with primary-transition energy $E_1 \approx 3$ –4 MeV falling into the continuous distribution, which is not resolved by the detectors in the form of individual peaks. Owing to the near-symmetry about half of the cascade energy in the intensity distributions obtained, this systematic error in determining the intensity sums can be acceptable for cascades with primary transitions $E_1 \lesssim 3$ MeV. Therefore, the conclusions following from analysis of the corresponding cascade intensities are quite correct.

In Figs. 6 and 13–18 the intensities of cascades to several low-lying levels of ^{146}Nd , ^{174}Yb , and ^{183}W are shown in the form of histograms as a function of their primary-transition energy.

The cascade intensities calculated using the first term in Eq. (1) are compared with experiment. The GEDR model with constant resonance width and two level-density models were used in the calculation. The crosses corre-

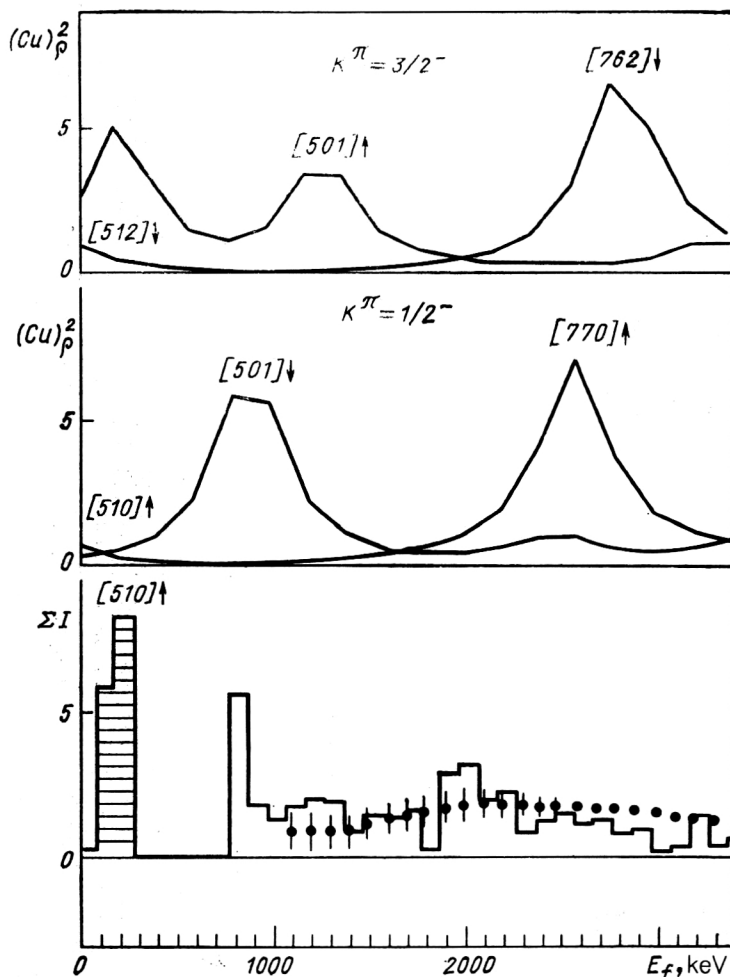


FIG. 11. The same for ^{187}W .

spond to the back-shifted Fermi-gas model, and the points correspond to the level-density model developed by A. V. Ignatyuk.

Both the calculated and the experimental intensities are given in percent per decay of a compound state and are determined independently of each other.

Comparison of the experimental and calculated intensities at various excitation energies of the compound nuclei ^{146}Nd , ^{174}Yb , and ^{183}W shows that it is impossible to make the shapes of the calculated and experimental distributions coincide using a simple model description of the properties of the excited states $E_i \lesssim B_n$.

In particular, along with the good agreement between the calculated and experimental intensities for small primary-transition energies ($E_1 < 2$ MeV) in these nuclei when the level-density model⁴ was used in the calculations, in several regions we observe a noticeable growth of the average widths of secondary $M1$ and $E2$ transitions (the most probable ones in these cases) to final low-lying levels of the compound nuclei. Such enhancement is absent for secondary transitions to levels up to $E_f \approx 1$ MeV (this question is studied in detail in Ref. 6; this is seen in Tables II and III).

The discrepancy between $I_{\gamma\gamma}^c$ and $I_{\gamma\gamma}^e$ noted above for cascades to different levels of the band of the state $[510]\uparrow$ in ^{183}W is seen in Figs. 16–18.

In a wide range of primary transitions (i.e., nuclear excitation energies) the widths Γ_{if} of transitions to the level $J^\pi = 3/2^-$ are smaller than those of transitions to the $1/2^-$ level, and this discrepancy is a maximum for transitions to the $5/2^-$ level.

This effect is not observed for the same band in ^{181}Hf . The nuclei ^{181}Hf and ^{183}W differ primarily in the value of $\Gamma_n^0/\langle\Gamma_n\rangle$ of resonances determining the cross section for thermal-neutron capture (see Fig. 7). In the case of ^{181}Hf transitions to states of few-quasiparticle nature are observed experimentally, while for ^{183}W transitions to collective states are observed. We have not found any other qualitative explanation of the observed effect.

4. DEPENDENCE OF THE CASCADE INTENSITY ON THE PRIMARY-TRANSITION ENERGY AND THE FUNDAMENTAL PARAMETERS OF γ DECAY

The spectral distribution (1) of the intensity of cascades between a compound state and a given low-lying level is a convolution of functions which are of interest for the theoretical description of nuclear properties.

These are the radiative strength function (RSF) of the primary transitions and the level density (LD) in a given range of variation of the quantum numbers corresponding to them. They can be extracted from the experimental dis-

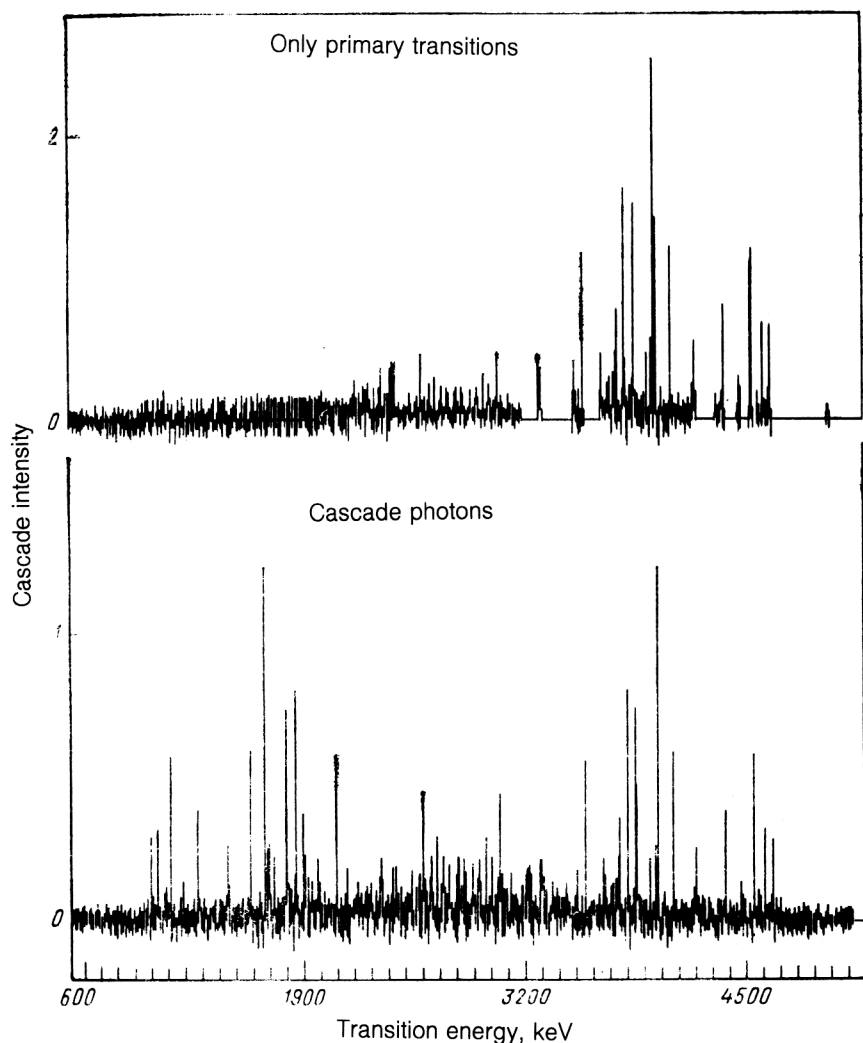


FIG. 12. An example of decomposition of the experimental distribution of cascades to the first excited state of ^{181}Hf (lower part) into components. The area of each spectrum is normalized to 100%.

tributions (see Figs. 1 and 4). This requires the following.

(1) In the measured distributions a fairly large fraction of intensity should be recorded from the primary transitions of compound-state decay. Experience shows that the practical threshold for this sum (including direct hard primary transitions to the final cascade levels) should be above 80% of Γ_λ (the full radiative width of the neutron resonance).

(2) The experimental distributions should be decomposed into two distributions corresponding to the first and second terms in Eq. (2).

(3) The full set of low-lying nuclear levels excited by $E1$ and $M1$ transitions should be known as completely as possible. Then, by a two-point approximation (using the neutron resonances and the low-lying states) the LD is specified in the entire range of energies $E_t < B_n$.

These conditions are necessary and sufficient at present for estimating the RSF in the entire range of E_1 studied in experiments, and the technique that we have developed, described in the preceding section, makes it possible to solve this problem (in principle) when studying neutron capture in any stable target nucleus.

In practice, the usefulness of a particular nucleus for determining the RSF is determined only by the technical

level of the experiment. Germanium detectors allow the determination of the RSF with about 10% efficiency in even-odd compound nuclei, in which the thermal-neutron capture cross section is determined by a resonance with $\Gamma_n^0 \gtrsim S_0 D_0$ for atomic masses in the range $137 \leq A \leq 181$, and most likely, it is broader. It may be possible to determine the RSF in even-odd nuclei with $\Gamma_n \ll S_0 D_0$ and also in even-even compound nuclei as soon as the detector efficiency is raised by a factor of 2–3 and/or systems of several nonresonance Ge detectors with efficiency of 20–30% and higher come into use.

In these cases it would be possible to experimentally obtain the intensity distributions of cascades from two successive transitions to several dozen final states of the nucleus in question.

Therefore, from the experimentally obtained distributions described by Eq. (1) we can obtain the dependence

$$\Delta I_{\gamma\gamma} = \sum_{i=1}^n \Gamma_{\lambda i}(E_\gamma) \Gamma_{if}(E_c - E_\gamma) / \Gamma_\lambda \Gamma_i \\ = \langle \Gamma_{\lambda i} \rangle \langle \Gamma_{if} \rangle \langle \rho_i \rangle \Delta E_i / \Gamma_\lambda \Gamma_b \quad (4)$$

which, in addition to the average transition widths and levels Γ , explicitly involves the density ρ_i of levels excited

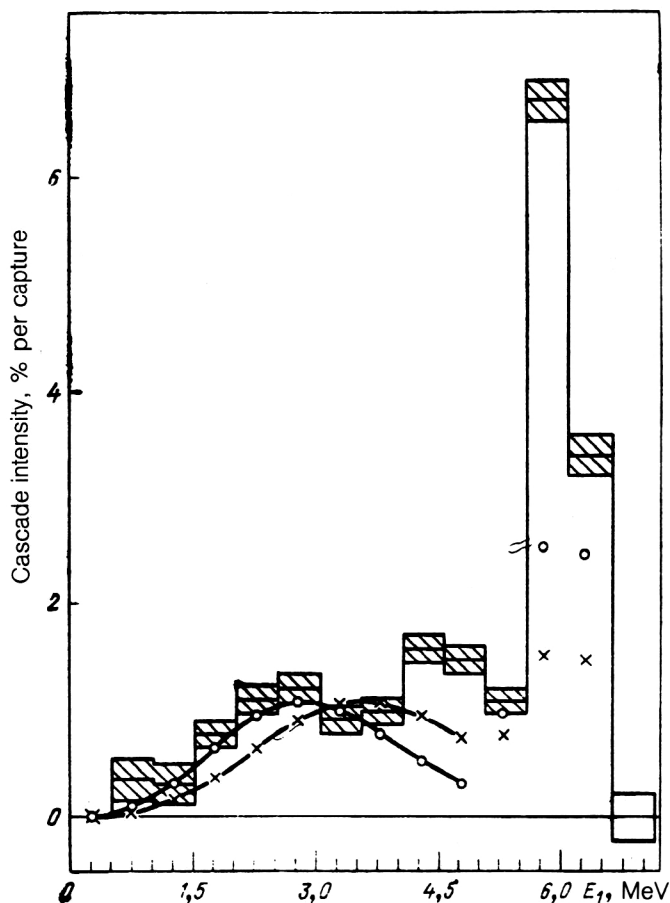


FIG. 13. Intensity distribution of cascades to the first excited state of ^{146}Nd . The notation is the same as that of Fig. 6.

by the primary transition E_γ . Summing over the set of experimentally observed final states of the cascades f , Eq. (4) can be brought to the form

$$\Delta I_{\gamma\gamma} = \langle \Gamma_{\lambda i} \rangle \kappa \langle \rho_i \rangle \Delta E_i / \Gamma_{\lambda}, \quad (5)$$

where the coefficient $\kappa = \sum_f \langle \Gamma_{if} \rangle / \Gamma_i \leq 1$ depends only on the number of final levels observed experimentally.

Actually, $\langle \kappa \rangle$ can exceed 0.8 in a large number of even-even targets, for which the reduced neutron width Γ_n^0 of the resonance determining neutron capture exceeds the average value $\langle \Gamma_n^0 \rangle$. These are nuclei in the range $137 \leq A \leq 181$ or an even wider range of atomic masses A .

It should be noted that κ depends on the energy of the primary transition: whereas for $E_1 \approx 0.5B_n$ in such nuclei κ must be practically 1, for $E_1 < 0.5B_n$ this coefficient must decrease with decreasing E_γ .

If in Eq. (5) we assume that $\kappa = 1$, then from the experimental data we can find a lower bound on the average value of the radiative width of the primary transition $\Gamma_{\lambda i}$:

$$\langle \Gamma_{\lambda i} \rangle \geq \Delta I_{\gamma\gamma} \Gamma_{\lambda i} / \langle \rho_i \rangle \Delta E_i. \quad (6)$$

Using the relation

$$K(E1) = \langle \Gamma_{\lambda i} \rangle / D_\lambda E_\gamma^3 A^{2/3}, \quad (7)$$

we can find a lower bound on the RSF of the primary transitions. Usually in experiments one obtains the sum of cascade intensities $I_{\gamma\gamma}$ for primary $E1$ and $M1$ transitions.

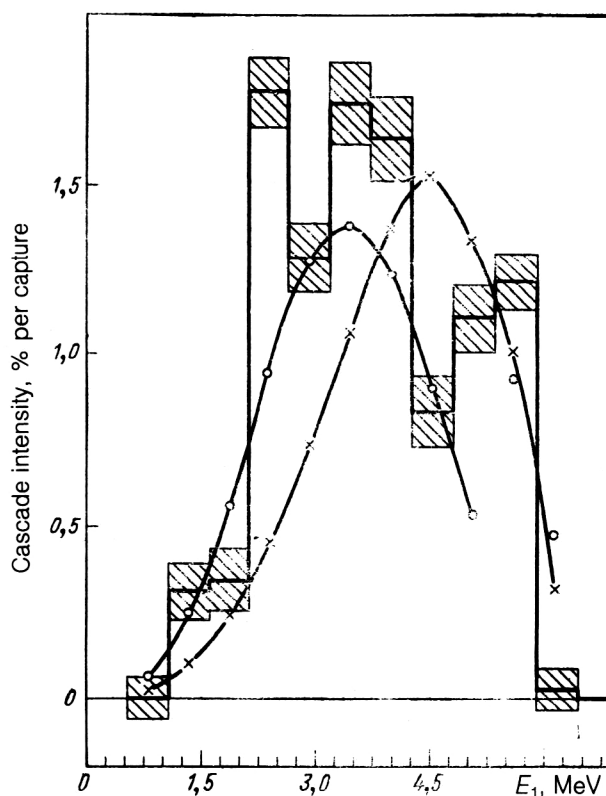


FIG. 14. Intensity distribution of cascades to the first excited state of ^{174}Yb . The notation is the same as that of Fig. 6.

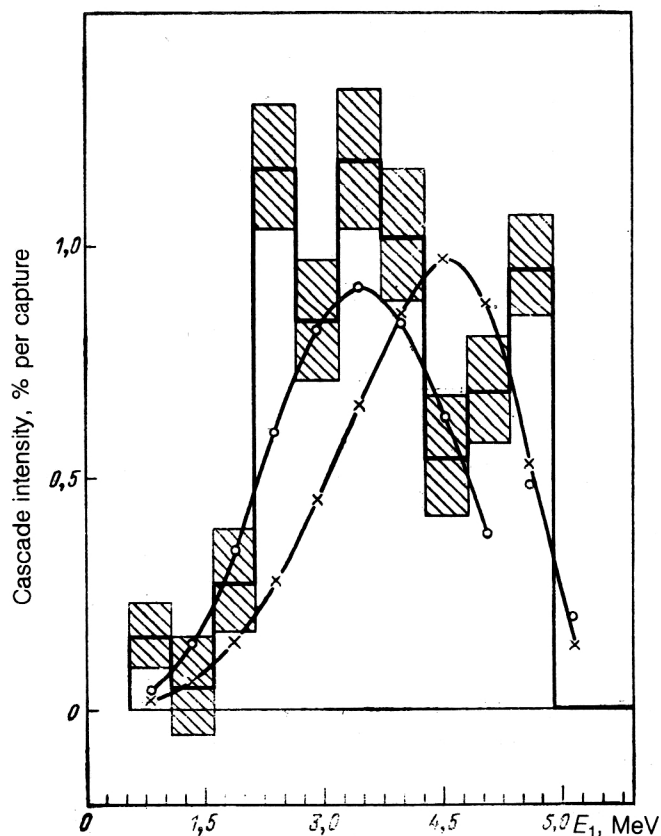


FIG. 15. Intensity distribution of cascades to the second excited state of ^{174}Yb . The notation is the same as that of Fig. 6.

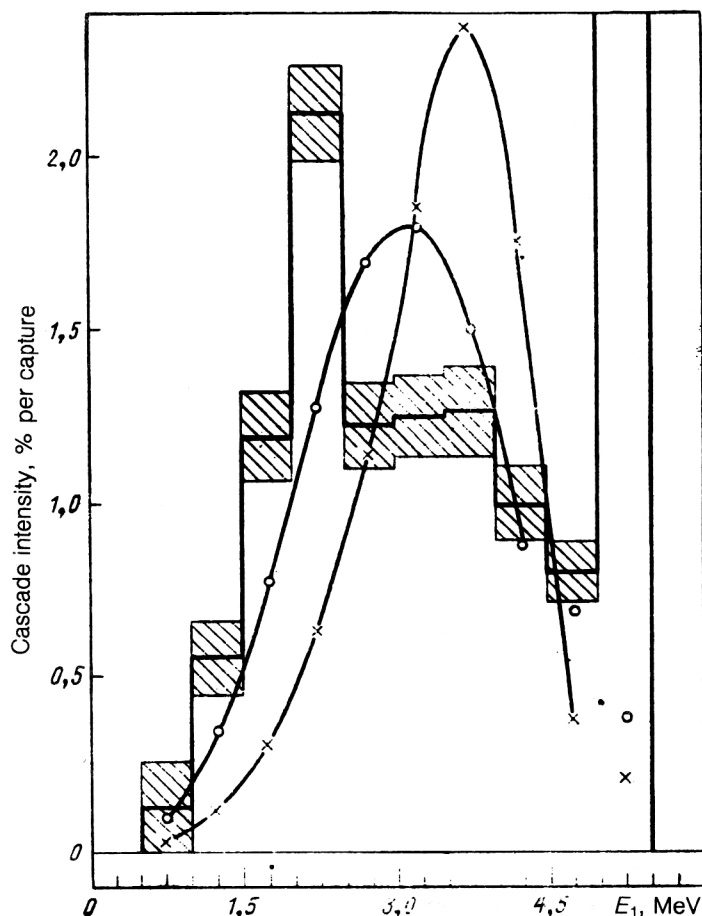


FIG. 16. Intensity distribution of cascades to the $1/2^-$ level of the ground-state band of ^{183}W . The notation is the same as that of Fig. 6.

If in Eq. (6) we use the value of $\langle \rho_i \rangle$ for only a single parity, then from Eq. (7) we will obtain a lower limit on the sum of the RSF of the $E1$ and $M1$ transitions.

Study of the reaction $(n, 2\gamma)$ on thermal neutrons gave rich spectroscopic information. The amount of such data certainly grows many times when studying cascades arising in the capture of neutrons with energy of about 2 keV and other energies in filtered beams. This follows directly from the fact that in capture in the region of the "averaged resonances" the fluctuations of the width $\Gamma_{\lambda t}$ decrease, and the fraction of primary transitions having intensity below 5×10^{-4} is decreased in relation to thermal-neutron capture. Here it also becomes possible in principle to separate the contributions of $E1$ and $M1$ transitions.

The possibility of determining the density of excited states in even-odd nuclei can be demonstrated for the example of ^{187}W . In Fig. 19 we show the growing sums of the number of experimentally observed states for $E_f > 1$ MeV and the predictions of the theoretical models. We see, for example, that the level-density model of Ignatyuk⁴ (curve 1) in this case predicts a considerably smaller density of excited states than that seen experimentally.

On the basis of the experimental level density we can obtain the parameters of the back-shifted Fermi-gas model. The fit was made for two extreme cases: when only states with $\pi = -1$ are observed experimentally (curve 3) and when states of both parities are observed (curve 2). In the comparison it should be remembered that the calculated

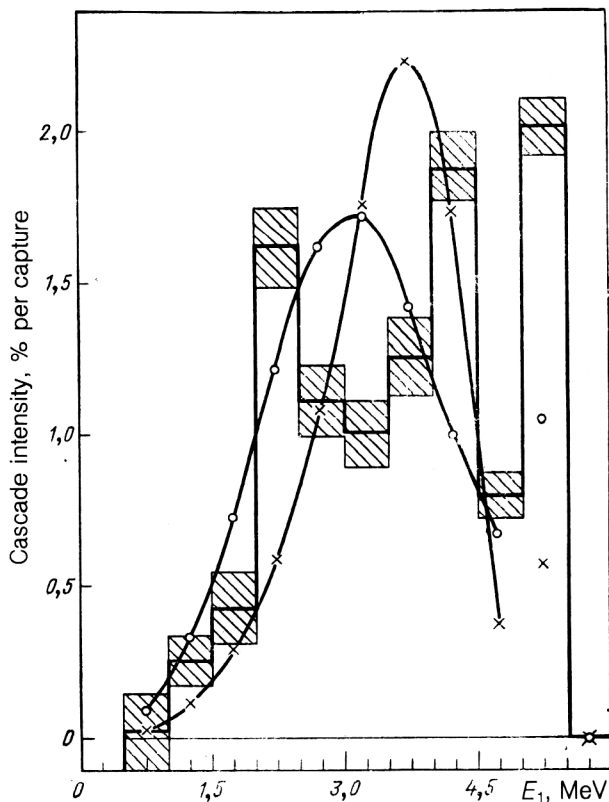


FIG. 17. Intensity distribution of cascades to the $3/2^-$ level of the ground-state band of ^{183}W . The notation is the same as that of Fig. 6.

level density (curve 2) is given only for the state with $\pi = -1$.

Assuming that the densities of states of both parities are identical, in this variant the doubled values of the growing sums of the number of levels agree fairly well with curve 3.

The good agreement between the shapes of the growing-sum curves obtained experimentally below 1.6–1.7 MeV allows us to state that all the levels excited by primary transitions of the dipole type in an even-odd nucleus can be established in this energy range. There are no fundamental restrictions on the further widening of this interval at the present time.

Estimates of the RSF have been obtained for the composite nuclei ^{173}Ba and ^{181}Hf . In Figs. 20 and 21 we show their intensities, summed over four and five final cascade levels, as functions of the primary-transition energy E_1 . The experiment was compared with the calculation for both variants of the energy dependence of the LD used above. (For ^{137}Ba they give almost the same results.)

It should be noted that here there is no complete and fairly good agreement between the experimental and calculated values of the cascade intensity. This confirms the conclusion drawn in the preceding section that the structures of the three states connected by the cascade affect the cascade intensity, since the calculation ignores this dependence.

The values of the RSF obtained on the basis of Eqs.

(6) and (7) for the studied nuclei are given in Figs. 22 and 23.

In the case of ^{137}Ba , $I_{\gamma\gamma} = (78 \pm 25)\%$ of Γ_λ . Here the error in the value of the total intensity of the experimentally observed primary transitions is mainly related to the uncertainty in the values of the cross section for thermal-neutron absorption in ^{136}Ba (Ref. 18) and, to a lesser degree, to the uncertainties in determining their absolute intensities.¹⁹

It is therefore not impossible that in the reaction $^{136}\text{Ba}(n,2\gamma)$ all the primary transitions of the decay of its compound state have been observed.

In the case of ^{181}Hf , $(80 \pm 4)\%$ of Γ_λ was isolated experimentally (52% for the cascade fraction and 28% for the fraction of direct transitions to five low-lying levels of ^{181}Hf).

In Figs. 20 and 21 we show the calculated sum $\Sigma\Gamma_{\lambda i}$ for these nuclei. The characteristic features of the distribution of this quantity—the center and width of the maximum—depend weakly on the details of the calculation. It can therefore be assumed that 20% of the intensity of primary transitions which are not observed experimentally in ^{181}Hf is related to primary transitions whose energy is below 2–2.5 MeV. If this 20% is distributed uniformly among transitions with $1 \leq E_1 \leq 2.5$ MeV, then it is possible to obtain an upper limit on the RSF in this interval (crosses in Fig. 23). The lower limit in both figures is given by the points.

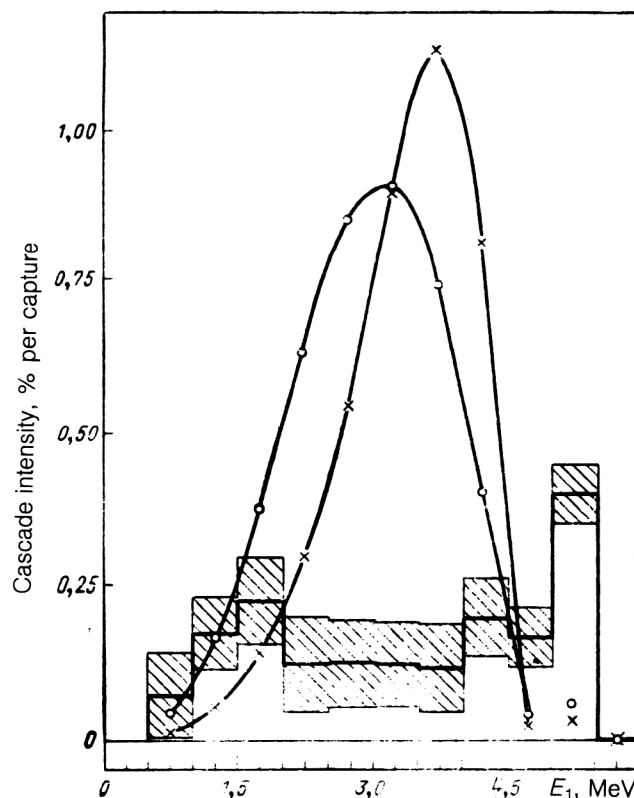


FIG. 18. Intensity distribution of cascades to the $5/2^-$ level of the ground-state band of ^{183}W . The notation is the same as that of Fig. 6.

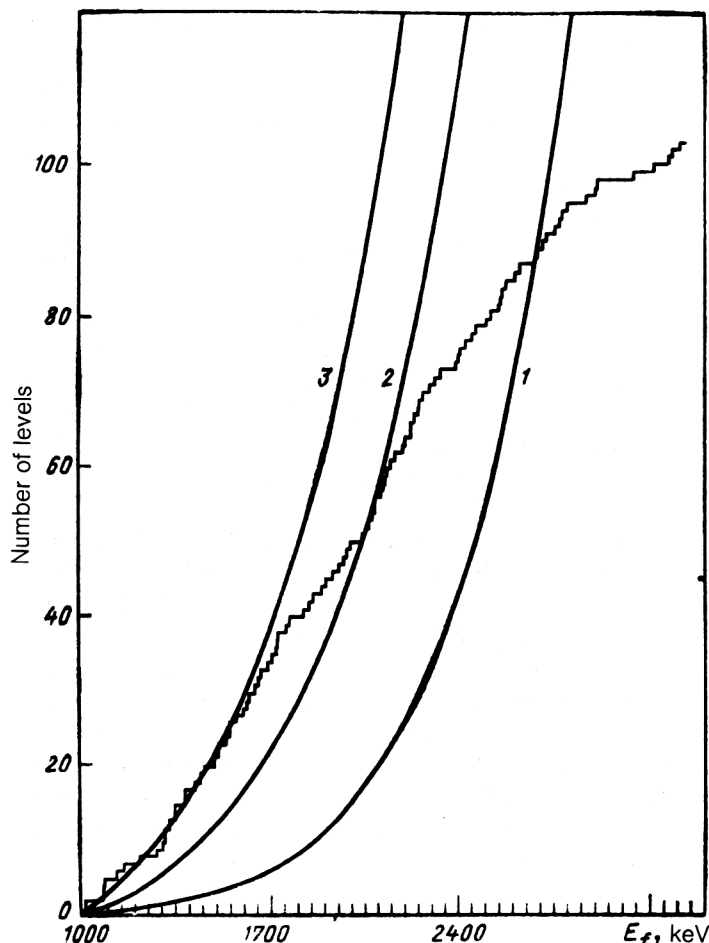


FIG. 19. Growing sums of experimentally observed (histogram) and predicted (only with $J^\pi = 1/2^-$ and $3/2^-$) numbers of excited states in ^{187}W as a function of the excitation energy E_f .

Comparison of the experimental estimates of the RSF and the theoretical predictions shows that the GEDR model [constant resonance width, Lorentz dependence of the cross section for the inverse reaction (γ, n)] gives a considerably worse description of experiment than the modified GEDR model,¹¹ which assumes that the resonance width depends on the nuclear temperature and the photon energy. The model of Ref. 11 was developed for a spherical nucleus. In the deformed nucleus ^{181}Hf we applied the approach of Ref. 11 to the parameters of the doubly peaked curve of the GEDR model independently of each other (assuming that the dependence of Ref. 11 is valid for both components of the GEDR).

Complete agreement between the experimental and calculated values of the RSF is also not obtained in this case, as can be seen from Figs. 22 and 23. The observed discrepancy can to some degree be explained by the following factors.

(a) Some of the widths could be enhanced owing to one-particle transitions between $4S$ and $3P$ neutron shells. Transitions with energy E_γ equal to 4742 and 4242 keV, which are responsible for the considerable growth of the RSF in ^{137}Ba , according to Ref. 19, excite the $3P_{1/2}$ and $3P_{3/2}$ states.

(b) $M1$ transitions could contribute to the value of the RSF found, since we are not in a position to determine the multipole order of the primary transitions.

(c) The level density ρ could be determined inaccurately. For transition energies $E_1 \lesssim 4$ MeV, owing to the absence of sufficiently reliable data on the excited-state schemes of ^{137}Ba and ^{181}Hf , we used the model density of states³ (ρ_i) with J^π equal to $1/2^-$ and $3/2^-$. If the densities of excited levels in these nuclei are predicted more accurately by the model of Ref. 4 (see Fig. 5), this could explain part of the discrepancy between the RSF found experimentally and calculated as in Ref. 11.

CONCLUSION

1. We have developed a technique for systematically studying the average parameters and features of the cascade γ decay of compound states of complex nuclei at excitations inaccessible to the traditional methods of analyzing this process.

2. We have established the presence of groups of primary transitions whose widths are correlated with the values of Γ_n^0 of compound states of even-odd nuclei of the $4S$ resonance of the neutron strength function, exciting levels above $E_i > 1$ MeV.

3. A very simple explanation of the features of the cascade decay of nuclei of this region has been obtained: the strong effect of one-particle transitions between the $4S$ and $3P$ shells on the partial widths of some of the primary transitions.

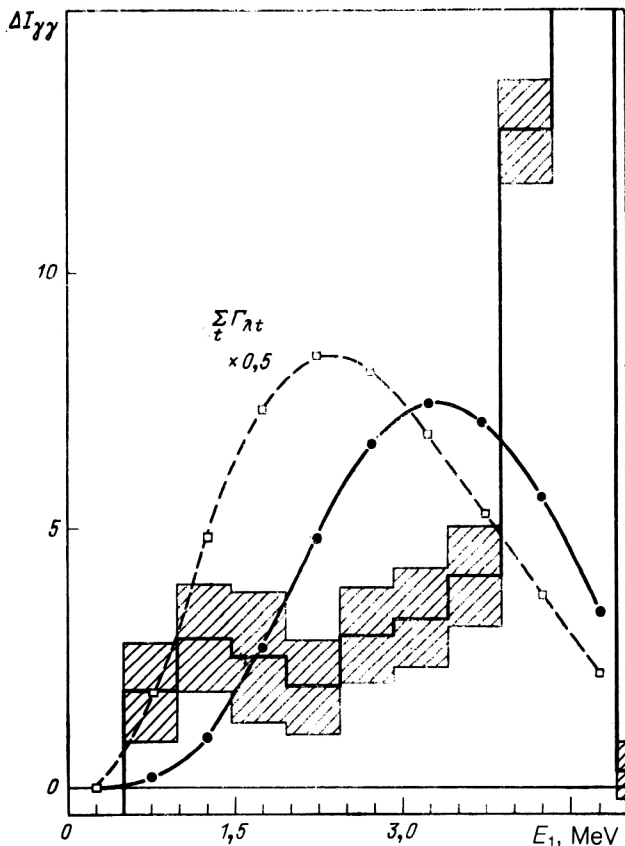


FIG. 20. Summed intensities of all cascades observed in the reaction $^{136}\text{Ba}(n,2\gamma)$ as a function of the primary-transition energy (% per decay): histogram—experiment; shaded region—error corridor (only statistical); solid line—calculation using the statistical theory; dashed line—calculated distribution of the sums $\Sigma\Gamma_{\lambda t}$ of partial widths of the primary transitions.

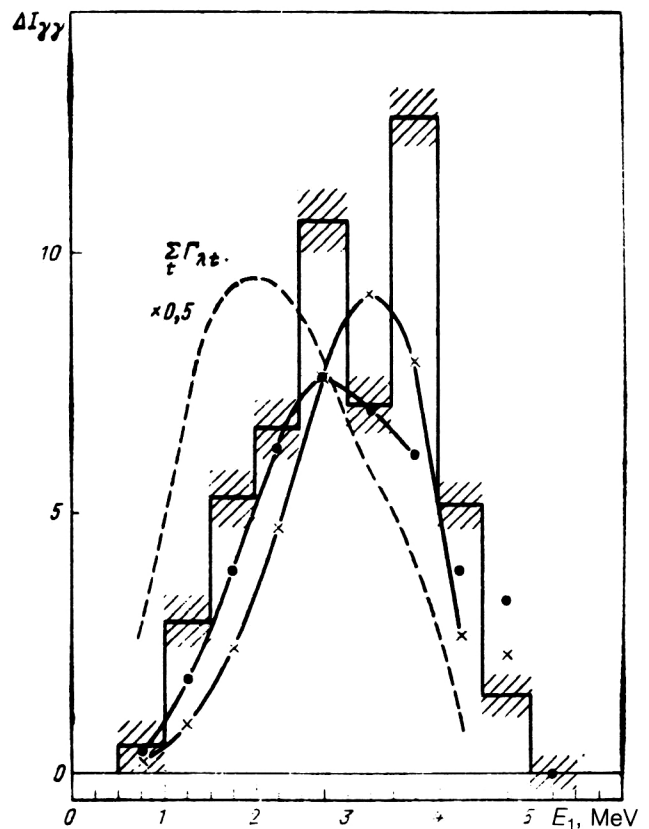


FIG. 21. The same as in Fig. 20 for ^{181}Hf . The points are calculated using the model of Ignatyuk, and the crosses are calculated using the back-shifted Fermi-gas model.

4. We have developed a technique and used it to estimate the RSF of soft primary transitions in the compound nuclei ^{137}Ba and ^{181}Hf .

5. We have found a class of nuclei in which the RSF can be estimated using a system of two Ge(Li) detectors: even-odd nuclei with Γ_n^0 of the compound state exceeding the average value.

6. We have proposed a simple hypothesis which explains the RSF dependence on the primary-transition energy as a superposition of one-particle transitions between the $4S$ and $3P$ neutron shells and transitions whose widths correspond to the GEDR model with width depending¹¹ on the γ frequency and the nuclear temperature. The proposed two-component RSF qualitatively describes the experimental results for both the spherical nucleus ^{137}Ba and the deformed nucleus ^{181}Hf .

7. To understand the γ -decay process it is necessary to further develop the technique for experimentally studying transition cascades in nuclei of various types. This is especially important for even-even deformed nuclei in the region of the rare-earth elements. It is particularly important to have detailed experimental and theoretical information about the role of enhanced $M1$ and $E2$ transitions at excitations $E_f = 2\text{--}4$ MeV, which are responsible for the con-

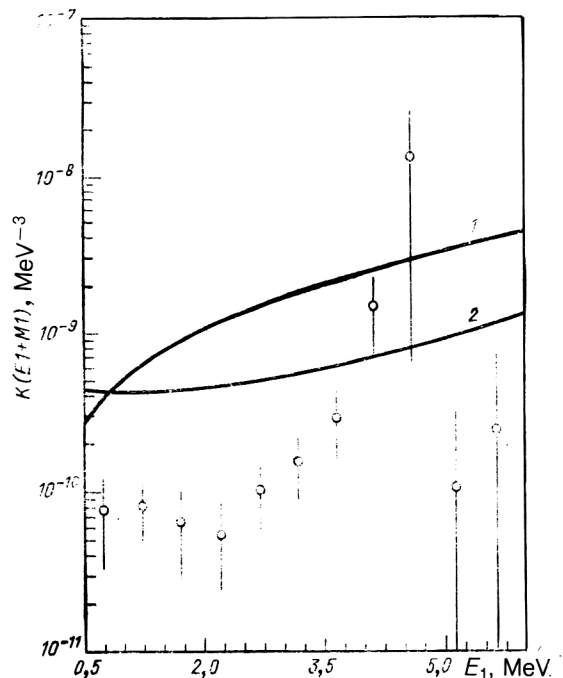


FIG. 22. Estimate of the RSF for ^{137}Ba . The errors include the uncertainty in the capture cross section and the statistical error in determining the intensities, and the Porter-Thomas fluctuations of the partial widths. Curve 1 is for the GEDR model with constant width, and 2 is for the GEDR model developed in Ref. 11.

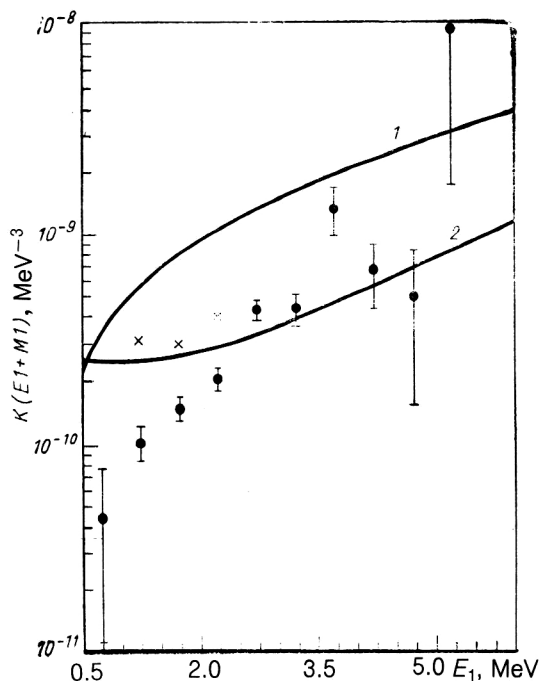


FIG. 23. Estimate of the RSF for ^{181}Hf . The crosses are the upper limit on the RSF estimated for soft ($E < 2.5$ MeV) transitions.

siderable excess of the experimentally observed cascade intensities over the model predictions. At present it is also very important to develop a sufficiently accurate model description of γ -decay processes in the entire transition region from relatively simple excitations to extremely complex compound systems.

¹S. T. Boneva, É. V. Vasil'eva, Yu. P. Popov *et al.*, *Fiz. Elem. Chastits*

- At. Yadra **22**, 479 (1991) [*Sov. J. Part. Nucl.* **22**, 232 (1991)].
- ²W. Dilg, W. Schantl, H. Vonach *et al.*, *Nucl. Phys.* **A217**, 269 (1973).
- ³V. G. Soloviev, *Theory of Complex Nuclei* (Pergamon, Oxford, 1976) [Russian original, Nauka, Moscow, 1971].
- ⁴A. V. Ignatyuk, *Statistical Properties of Excited Nuclei* [in Russian] (Énergoatomizdat, Moscow, 1983).
- ⁵A. I. Vdovin, V. V. Voronov, L. A. Malov *et al.*, *Fiz. Elem. Chastits At. Yadra* **7**, 952 (1976) [*Sov. J. Part. Nucl.* **7**, 380 (1976)].
- ⁶É. V. Vasil'eva, Yu. P. Popov, A. M. Sukhovoï *et al.*, *Yad. Fiz.* **44**, 857 (1986) [*Sov. J. Nucl. Phys.* **44**, 552 (1986)]; S. T. Boneva, V. A. Khitrov, Yu. P. Popov *et al.*, *Z. Phys. A* **330**, 153 (1988).
- ⁷N. P. Balabanov, V. A. Vtyurin, Yu. M. Gledenov *et al.*, *Fiz. Elem. Chastits At. Yadra* **21**, 317 (1990) [*Sov. J. Part. Nucl.* **21**, 131 (1990)]; Yu. Andzheevskii, Vo Kim Than, V. A. Vtyurin *et al.*, Report R3-81-433, JINR, Dubna (1981) [in Russian].
- ⁸O. Frehers, D. Bohle, A. Richter *et al.*, *Phys. Lett.* **218B**, 439 (1989).
- ⁹S. T. Boneva, É. V. Vasil'eva, V. D. Kulik *et al.*, *Izv. Akad. Nauk SSSR Ser. Fiz.* **54**, 836 (1990) [*Bull. Acad. Sci. USSR Phys. Ser.*].
- ¹⁰S. F. Mughabghab, *Neutron Cross Sections* (Academic, New York, 1984), Vol. 1, Part B.
- ¹¹S. G. Kadenskii, V. P. Markushev, V. I. Furman *et al.*, *Yad. Fiz.* **37**, 277 (1983) [*Sov. J. Nucl. Phys.* **37**, 165 (1983)].
- ¹²S. T. Boneva, V. A. Khitrov, A. M. Sukhovoï, and A. V. Vojnov, Preprint E3-90-45, JINR, Dubna, 1990.
- ¹³F. A. Gareev, S. P. Ivanova, V. G. Solov'ev *et al.*, *Fiz. Elem. Chastits At. Yadra* **4**, 357 (1973) [*Sov. J. Part. Nucl.* **4**, 148 (1973)].
- ¹⁴L. A. Malov and V. G. Solov'ev, *Yad. Fiz.* **26**, 729 (1977) [*Sov. J. Nucl. Phys.* **26**, 384 (1977)]; *Nucl. Phys.* **A270**, 87 (1976).
- ¹⁵S. T. Boneva, É. V. Vasil'eva, L. A. Malov *et al.*, *Yad. Fiz.* **49**, 944 (1989) [*Sov. J. Nucl. Phys.* **49**, 587 (1989)]; S. T. Boneva, V. A. Khitrov, L. A. Malov *et al.*, in *Proc. of the 23rd Yamada Conf.*, Osaka, Japan, 1989 (World Scientific, Singapore, 1989), p. 372.
- ¹⁶S. T. Boneva, É. V. Vasil'eva, and A. M. Sukhovoï, *Izv. Akad. Nauk SSSR Ser. Fiz.* **51**, 1923 (1987) [*Bull. Acad. Sci. USSR Phys. Ser.*].
- ¹⁷S. T. Boneva, É. V. Vasil'eva, Yu. P. Popov *et al.*, *Izv. Akad. Nauk SSSR Ser. Fiz.* **52**, 2082 (1988) [*Bull. Acad. Sci. USSR Phys. Ser.*].
- ¹⁸L. Koester, K. Knopf, and W. Waschowski, *Z. Phys. A* **322**, 105 (1985).
- ¹⁹L. V. Groshev, V. N. Dvoret'skii, A. M. Demidov, and M. S. Al'vash, *Yad. Fiz.* **10**, 681 (1969) [*Sov. J. Nucl. Phys.* **10**, 392 (1969)].

Translated by Patricia Millard